



This is a repository copy of *A novel powder-epoxy towpregging line for wind and tidal turbine blades*.

White Rose Research Online URL for this paper:

<https://eprints.whiterose.ac.uk/210445/>

Version: Accepted Version

Article:

Robert, C. orcid.org/0000-0001-5035-6134, Pecur, T. orcid.org/0000-0003-2267-1115, Maguire, J.M. et al. (3 more authors) (2020) A novel powder-epoxy towpregging line for wind and tidal turbine blades. *Composites Part B: Engineering*, 203. 108443. ISSN 1359-8368

<https://doi.org/10.1016/j.compositesb.2020.108443>

Article available under the terms of the CC-BY-NC-ND licence (<https://creativecommons.org/licenses/by-nc-nd/4.0/>).

Reuse

This article is distributed under the terms of the Creative Commons Attribution-NonCommercial-NoDerivs (CC BY-NC-ND) licence. This licence only allows you to download this work and share it with others as long as you credit the authors, but you can't change the article in any way or use it commercially. More information and the full terms of the licence here: <https://creativecommons.org/licenses/>

Takedown

If you consider content in White Rose Research Online to be in breach of UK law, please notify us by emailing eprints@whiterose.ac.uk including the URL of the record and the reason for the withdrawal request.



eprints@whiterose.ac.uk
<https://eprints.whiterose.ac.uk/>

A novel powder-epoxy towpregging line for wind and tidal turbine blades

Colin Robert*, Toa Pecur, James M. Maguire,

Austin D. Lafferty, Edward D. McCarthy, Conchúr M. Ó Brádaigh

School of Engineering, Institute for Materials and Processes, The University of Edinburgh,
Sanderson Building, King's Buildings, Edinburgh, EH9 3FB, UK

*Corresponding author

Keywords: Powder-epoxy, towpregging, joule heating, carbon fibres, basalt fibres, hygrothermal ageing

Highlights:

- The powder-epoxy towpregging process was described in detail for both carbon fibres and basalt fibres.

- Excellent static mechanical properties were reported for unidirectional carbon-fibre/powder-epoxy composites and the influence of fibre volume fraction (FVF) was analysed.

- Two types of basalt fibre were tested, showing comparable mechanical properties to glass fibre composites.

- A hygrothermal study of both carbon-fibre composites and basalt-fibre composites showed that the latter had a greater sensitivity to water uptake and immersed ageing.

Abstract

A novel material and process was developed using fibre-reinforced powder-epoxy to produce unidirectional towpreg with a pilot-scale towpregging line, for cost-effective production of large composite structures for the renewable energy market, specifically for wind and tidal turbine blades. Electrostatic attraction was used to coat fibre tows with powder epoxy and either joule or radiant heating employed to heat and melt the polymer, followed by consolidation between rollers. Unidirectional carbon-fibre and basalt-fibre reinforced polymer laminates (UD-CFRP and UD-BFRP, respectively) were manufactured from the towpreg. Tensile test results showed that the towpregging process could be employed to achieve high performance UD-CFRP with 0° tensile properties that are similar or better than commercially-available UD-CFRP systems. The competitive advantages of the powder-epoxy towpreg system include lower cost, better overall manufacturing control for vacuum-bag-only manufacturing and the ability to co-cure parts together at a later stage. Mechanical test results showed some variation between two types of UD-BFRP, but the results compared well with published data on UD-BFRP and equivalent glass-fibre reinforced polymer (GFRP) systems. Finally, the influence of hygrothermal ageing due to water immersion on the tensile properties of the materials was investigated, with tests revealing that the water ageing effect was more severe in the case of UD-BFRP than for UD-CFRP.

1. Introduction

The International Energy Agency has reported an increasing rate of electricity generation worldwide of 8.28% per year over the last 50 years [1], which has been accelerating in the last two decades to sustain emerging economies. Despite a rapid expansion of renewable energy sources in the past 20 years [2], the overall contribution of renewable energy is still modest (1.8% for wind and solar, 2.5% for hydro) in comparison to global energy consumption. In this regard, optimisation and diversification of renewable energy sources and technologies have become paramount. Ocean energy potential, although very substantial at an estimated 8,000 TWh/year [3], is still largely under-exploited.

To exploit the full potential of offshore energy, in particular, several significant challenges must be addressed for wind and tidal turbine composite structures. These structures operate in severe environments undergoing high fatigue loading, water ingress, erosion, immersed ageing, bio-fouling, etc. [4–8]. Accordingly, the composite structures must have high mechanical properties, which cannot degrade significantly over the lifespan of the device (approx. 20 – 25 years). GFRP has been used predominantly in the manufacture of wind and tidal turbine blades due to its good mechanical performance, relatively low cost, and formability for complex geometries. As these blades get larger, however, the demand on mechanical performance increases, along with the need to lower the levelised cost of energy (LCOE).

For several years, basalt fibres have been investigated as a potential alternative to glass fibres; in particular, for E-glass fibres, which are widely used by the composites industry [9,10]. Basalt fibres are reported to have similar mechanical properties to S-glass fibres, however, the basalt fibre production requires less energy and less additives than glass fibre production [11], meaning that it costs less than S-glass [10]. In general, it has been shown in the literature that BFRP has mechanical properties which are comparable to, if not higher than, GFRP [11,12]; albeit, with considerable variation in reported properties. Some of this variation may be linked to basalt being from a natural source with a chemical composition that depends on location, as well as the typical variations between suppliers ascribed to their production methods [10]. In this regard, BFRP has not had the same level of evaluation as GFRP and CFRP to build a comprehensive knowledge of its mechanical behaviour. In the context of this paper, there are few studies which have documented the immersed performance of BFRP for marine applications [13–15]. Nevertheless, basalt fibre technology continues to advance, and the aforementioned studies reported sufficiently promising results to warrant further investigation as a potential alternative to GFRP for wind and tidal turbine blade manufacture.

Where higher performance materials are required, CFRP has also been investigated as an alternative to GFRP due to its high specific strength and stiffness. To maintain a low LCOE, however, careful consideration of blade design is required to optimise the cost effectiveness of introducing CFRP [16]. Many wind turbine blade manufacturers have implemented hybrid composite designs to offset the associated costs [4,6,17–21] (e.g. a CFRP spar with a GFRP root, shear web, and skins). As the main load bearing sub-structure along the span of the blade, the spar must withstand significant tensile and compressive stresses. Consequently, spars are very thick unidirectional laminates. Depending on the blade size and design, the spar may taper from 150 mm thickness down to less than 5 mm [6,22]. For wind turbines, this occurs over a larger span (e.g. 70 m) than for tidal turbine blades (e.g. 8.5 m). The spar caps for a 2 MW tidal turbine blade can taper from 104 mm thickness to 25 mm [23]. Manufacturing such laminates poses several processing challenges including maintaining fibre alignment and straightness [24], difficulty infusing with conventional methods (such as vacuum-assisted resin transfer moulding (VaRTM)) [6], and difficulty in controlling the exothermic curing reaction of the resin matrix [25]. Accordingly, several material suppliers have developed UD-CFRP vacuum-bag-only (VBO) prepregs specifically aimed at manufacturing spars and similar structures for

1 wind and tidal turbine blades; Gurit's SparPreg™, Hexcel's Hexply M9.6 series and M79 prepreg, and
2 Cytec's (formerly ACG's) VTM 260 series [4]. The advantages of these VBO prepregs is that they greatly
3 reduce the complexity of the infusion process as they are supplied in a partially or fully impregnated
4 form. Their disadvantage is that they typically require temperature-controlled storage to prevent
5 premature curing of the resin system (i.e. out-time effects [26]), and they generally do not address
6 the issue of high exotherms, with the exception of Hexcel's Hexply M79 resin [27]. One alternative
7 that allows blade manufacturers to avoid infusing dry fabric and controlling large exotherms, is the
8 use of pultruded UD-CFRP [18,20,28], which has even been considered for offshore wind turbine tower
9 structures [29]. Pultruded sections are fully infused (usually to a relatively high fibre volume fraction)
10 and they are typically pre-cured, so they have no exotherm, they don't require temperature-
11 controlled storage, and their high degree of fibre alignment is "locked in". The major disadvantage
12 with these fully-cured pultruded sections is that they are difficult to form to complex geometries, such
13 as the double curvatures in turbine blades, and they must be adhesively bonded together to form a
14 single spar.

15 The technology described in this paper aims to address the aforementioned disadvantages of
16 conventional VBO prepregs and pultruded sections by utilising the unique properties of a novel
17 powder-epoxy matrix. In relation to fibre-reinforced composites, this powder-epoxy has been the
18 subject of several studies in recent years which have investigated its processing behaviour [30–32], its
19 mechanical behaviour [33–35], its behaviour in immersed conditions [36], and its application in wind
20 [17] and tidal turbine blades [23,37]. Powder-epoxies, along with other thermosetting powders, are a
21 commodity product from the coatings industry, which are widely available in bulk from a range of
22 suppliers (e.g. FreiLacke, DSM, AkzoNobel, 3M, etc.). These powders tend to have excellent storage
23 stability due to a high initial glass transition temperature (around 40°C) [38] and the frequent use of
24 heat-activated latent curing agents in their formulation [39]. This means they can be used to make
25 VBO prepregs which do not require temperature-controlled storage and generate significantly less
26 exotherm than conventional epoxy systems [30,32]. Moreover, due to the processing stability of the
27 powder-epoxy [30], it has been shown that sub-components (e.g. turbine blade skins) can be infused
28 at 120°C, cooled to ambient conditions to form solid β -staged preforms (i.e. partially cured),
29 assembled together, and then co-cured at 180°C [40]. The ability to store powder-epoxy preforms for
30 use at a later stage is a strong competitive advantage of this technology. The ability to then co-cure
31 these pre-formed parts is also very interesting, especially for the wind industry where blades are
32 usually manufactured in sections and then adhesively bonded. The new process can thus avoid an
33 extra processing step while maintaining the mechanical properties at the joining line, which can
34 sometimes be design-critical.

35 The powder-epoxy is used in this study for the production of 'towpreg' a.k.a. pre-impregnated tows.
36 In short, this production process consists of spreading the fibres of a tow, depositing powder between
37 the fibres, heating the coated fibres, and then consolidating them. Spanning the last four decades,
38 towpregging has been investigated by several authors for both thermoplastics and thermosets [41–
39 45]. It has been shown that this production route has benefits over hot melt prepregging and solution
40 prepregging in terms of cost and environmental impact; including little or no volatile organic
41 compounds (VOCs) and little waste disposal due to powder reclamation and reuse [46]. Towpreg can
42 be used for automated tape placement (ATP); either as a single towpreg (a.k.a. automated fibre
43 placement (AFP)) or several consolidated towpreg (a.k.a. automated tape laying (ATL)) [44,47]. It can
44 also be used in pultrusion [42,48] or filament winding [45]. This versatility lends itself to many
45 industrial applications, however, to the authors knowledge there is little or no evidence to suggest it
46 has been applied to the production of wind or tidal turbine blades or structures.

1 Initial work has been carried out on developing a pilot-scale powder towpregging for the
2 aforementioned application [49,50]. In this study, a more mature version of the pilot powder
3 towpregging line is described. Both carbon-fibre towpreg and basalt-fibre towpreg are investigated as
4 alternatives to GFRP systems. Mechanical testing is carried out on UD-CFRP laminates made from the
5 CF towpreg and compared with existing data to determine if the towpregging process has an adverse
6 effect on the mechanical performance of the carbon fibres. The influence of fibre volume fraction, and
7 its variability with respect to the towpregging line, is also studied for carbon-fibre towpreg. UD-BFRP
8 laminates are made using basalt fibres from two different suppliers. These laminates are mechanically
9 tested to study the variation between suppliers. Mechanical results for UD-BFRP are also compared
10 with published data on equivalent material systems. Finally, a hygrothermal ageing study is carried
11 out on UD-CFRP and UD-BFRP to assess the performance of both materials in immersed conditions.

12

13 2. Materials

14

15 2.1. Terminology

16 In the literature relating to material development and material production, the term ‘towpreg’ has
17 been used commonly to describe tows that are impregnated with a thermoset powder or a
18 thermoplastic powder [44,51,52]. For clarity, in this work, ‘tow’ is used to refer to the unimpregnated
19 tow, and ‘towpreg’ is used for one or more tows that have been impregnated with powder and then
20 sintered and consolidated, but which are still uncured. This terminology is chosen because ‘towpreg’
21 represents a highly versatile precursor material which can later be developed for numerous
22 manufacturing processes including pultrusion, ATP, filament winding, etc.

23

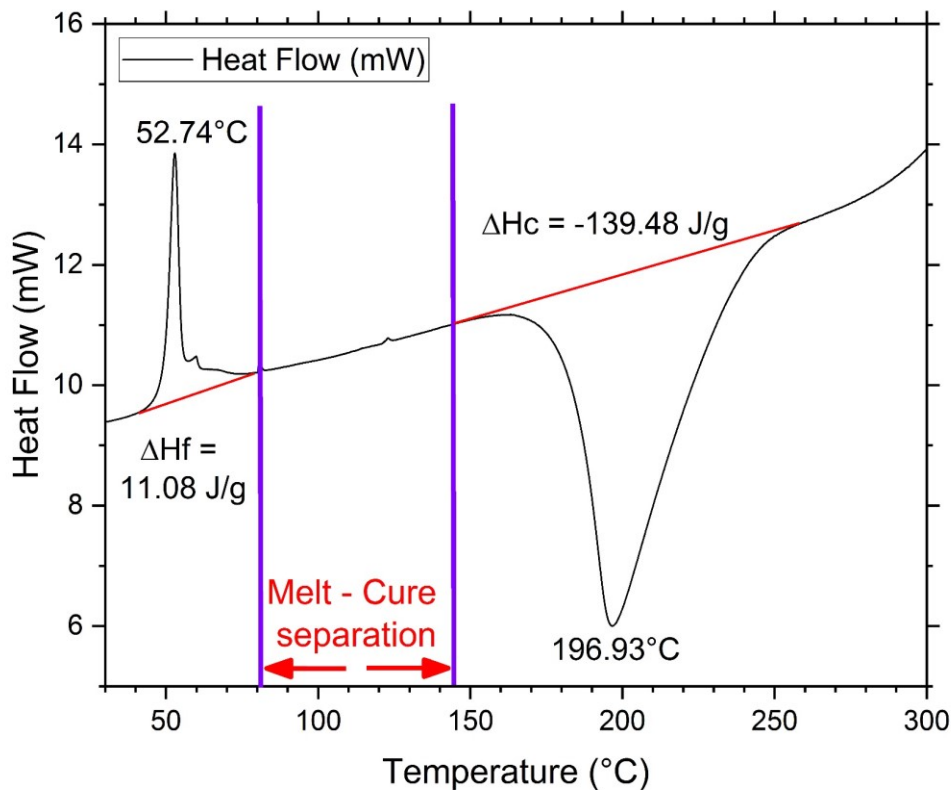
24 2.2. Powder-epoxy

25 All the composites in this study were manufactured using a novel powder-based epoxy matrix. The
26 powder-epoxy (PE6405, density 1220 kg/m³) was engineered by Swiss CMT and then produced by
27 FreiLacke. The processing characteristics of the powder-epoxy can be defined by two steps, which are
28 relevant to both towpreg production and laminate manufacturing:

- 29 a) The powder-epoxy melts and sinters at around 40-60°C, reaching a minimum viscosity for
30 infusion around 120°C.
- 31 b) The curing is then carried out through a heat activated catalytic process where the curing
32 agent requires a temperature of at least 145°C for reaction initiation, as described by Maguire
33 et al. [30] and Mamalis et al. [33] and shown by differential scanning calorimetry (DSC) in
34 Figure 2.

35 The details of the chemistry involved are proprietary to the manufacturers of these commercially
36 available products. The powder-epoxy has numerous advantages compared to standard VBO prepreg
37 systems when building large, thick -section structures such as the latest wind turbine blades (over 100
38 mm thickness at the blade root). Firstly, the low melt viscosity (minimum of 1.26 Pa.s [30]) and low
39 rate of cure below 120°C allows more time to fully infuse the section [30–32]. Secondly, as shown in
40 Figure 1, the powder-epoxy, PE6405 displays a curing exotherm of approx. 140 J/g, which is less than
41 a third of the enthalpy of standard liquid resin epoxy systems (about 500 J/g) [30]. This feature is
42 crucial in reducing the risk of thermal runaway for thick section composites manufacturing which
43 allows for quicker production rates [31,32].

1 Figure 2 also highlights the powder-epoxy's ability to separate the melting/sintering phase (ending at
 2 80°C) from the curing phase (starting at 145°C). Since the PE6405 melting/sintering temperature is
 3 considerably lower than the curing temperatures, composite parts can be impregnated in one stage,
 4 and then cured in another. For this reason, a two-stage heating profile is typically used as presented
 5 in Figure 2. As previously mentioned, this feature gives manufacturers the ability to reform and co-
 6 cure complicated parts as necessary. This strongly increases the cohesion of the different parts and
 7 removes the need for an extra adhesion step, thus allowing 'one-shot' manufacturing, as shown in
 8 Figure 3 [40,53,54].

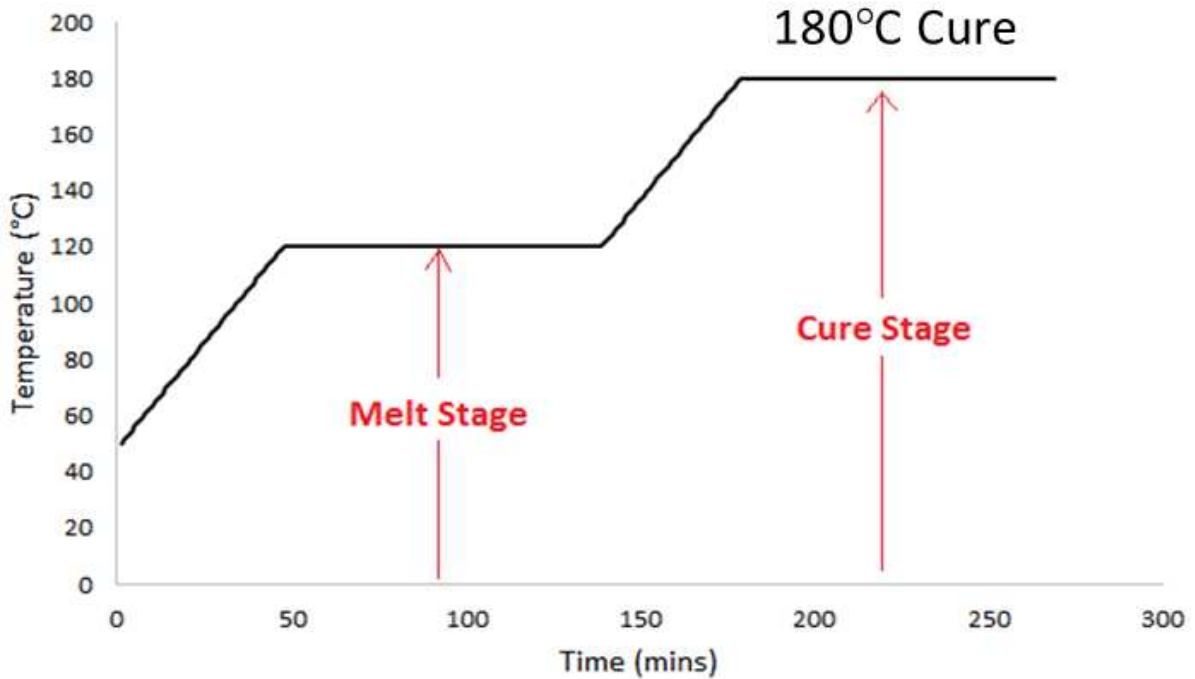


9
 10 **Figure 1: DSC data showing a temperature sweep (20°C/min) of neat powder-epoxy sample,**
 11 **exhibiting peaks due to a reversal of enthalpic relaxation (at 52.74°C) and curing (at 196.93°C). The**
 12 **temperature gap between the end of the melting/sintering and the beginning of the cure is**
 13 **represented by the purple lines. Note: exotherm is downwards.**

14
 15 In recent times, 'one-shot' manufacturing processes have been targeted by both the wind and tidal
 16 energy industries due to the added cost and weight of adhesives, as well as the potential for adhesive
 17 bondlines to act as 'weak spots' in the structure [5,55]. These reported technologies all utilise some
 18 form of VaRTM process to manufacture their 'one-shot' structures, but as Harper et al. [5]
 19 acknowledge, it is unclear whether such processes can be used to successfully thick sections in 'one-
 20 shot' (due to exotherms and difficulty infusing), or whether thick-section parts must be prefabricated
 21 and later introduced during infusion of the skins [55]. In contrast, the low-exotherm powder-epoxy
 22 'one-shot' technology can be used with VBO prepreg materials, thus reducing the risk of poor infusion
 23 or 'thermal runaway'.

1 One limitation to the powder-epoxy technology is that the heat-activated curing agent requires higher
2 temperatures for curing (> 160°C) than what is typical for conventional processes like VaRTM.
3 Nevertheless, integrally-heated ceramic tooling has been developed to achieve the required
4 processing conditions, and was used to produce “one-shot” 12.6m wind turbine blades, shown in
5 Figure 3, using glass-fibre/powder-epoxy VBO prepregs [40].

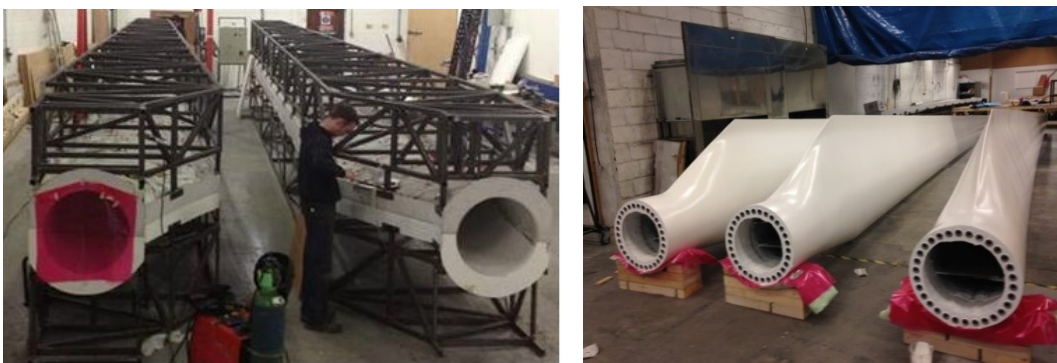
6



7

8 *Figure 2: Typical melting and cure cycle for processing of powder-epoxy composites. Powder-epoxy*
9 *composites can be melted and consolidated at 110-120°C without any significant curing, thus*
10 *allowing individual components to be consolidated and assembled for a final co-cure at 180°C.*

11



12

13 *Figure 3: Ceramic heated tools (left); and 12.6 m blades made from powder-epoxy based VBO*
14 *prepreg (right) [39]*

15

16 2.3. Carbon fibres

17 Mamalis et al. investigated the influence of sizing and fibre straightness on the mechanical properties
18 of PE6405 powder-epoxy reinforced with Toray T700S-24K carbon fibres (CF) [33,35]. In their studies,

1 it was found that fibre straightness had a significant effect on mechanical properties, and the 50C sized
 2 CF were found to be superior compared to two other fibre sizings. As such, T700S-24K-50C fibres
 3 (equivalent to 1650 Tex) from Toray Industries Inc. [56] were chosen for this study; with individual
 4 fibres having a diameter of 11 μm .

7 2.4. Basalt fibres

8 Variation in basalt fibre (BF) quality between different suppliers is common, as basalt is naturally
 9 sourced from volcanic rocks, producing different chemical compositions when forming [11]. The
 10 precise details of fibre manufacturing and sizing processes are often kept confidential, which leads to
 11 greater uncertainty on the quality and reproducibility of the fibres. To address these concerns, the
 12 properties of two different commercially available basalt fibres were investigated and compared in
 13 this study; BF from Basaltex [57,58], and BF from Mafic [59]. Both Mafic BF and Basaltex BF had a fibre
 14 diameter of 13 μm , and were supplied in the form of 2400 Tex assembled rovings. The fibres were
 15 both coated in alkoxysilane sizing, usually used in glass fibres for optimal cohesion with epoxide
 16 systems [58,59]. A comprehensive summary of fibres and matrix mechanical properties are presented
 17 in the table below.

18 **Table 1: Individual mechanical properties of fibres and powder epoxy matrix**

	σ_M (MPa)	E (GPa)	ϵ_f (MPa)	Diameter (μm)	Density (g/cm^3)
T700s carbon fibres [56]	4900	230	2.1	7	1.81
Mafic [®] direct roving [59]	3100	88-92	3.5	13	2.63
Basaltex [®] direct roving [58]	2900-3100	85-89	3.5	13	2.67
PE6405 from Freilacke [®] [35]	73.1	3.0	2.43*	N/A	1.22

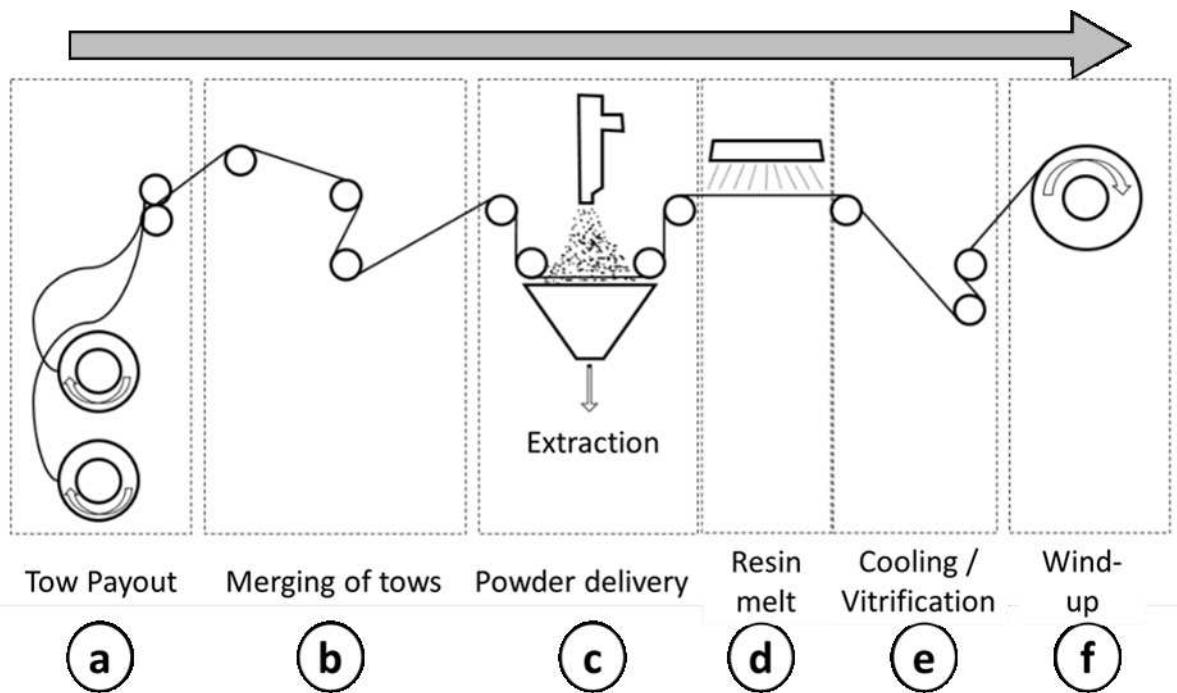
20 * linear elastic behaviour assumed

22 3. Towpregging process

24 3.1. General description of the towpregging line

25 The pilot towpregging line was designed and constructed based on existing designs from the literature,
 26 such as the thermoplastic towpregging developed by Edie et al. [41]. Figure 4 represents the different
 27 steps of the process; all of which have an effect on the final properties of the towpreg. These steps
 28 are briefly described below to give a general understanding of the towpregging line, prior to going into
 29 further detail in the next sections.

- 1 a) The tows were guided through steel rings and tensioned with two interlocked
- 2 Polytetrafluoroethylene (PTFE) rollers.
- 3 b) Extra tension was applied using two additional PTFE rollers and the tows were merged by a
- 4 chamfered roller.
- 5 c) The fibres were pulled through the deposition chamber where an electrostatic spray gun
- 6 deposited powder particles onto the fibres at a 90° angle.
- 7 d) Heat was applied to the powder-coated fibres via an energy source tailored to the fibre type
- 8 in order to melt the powder.
- 9 e) The towpreg was cooled in ambient air under tension.
- 10 f) Finally, the vitreous towpreg was wound-up on a drum, which was motorised to keep the
- 11 whole line under tension.



12
13 **Figure 4: Towpregging line schematic. The arrow indicates the direction in which the tow is**
14 **travelling.**

15
16 **3.2. Tow payout**

17 Tow payout for this study involved two tows being unwound from the as-supplied material drum while
18 under tension. The payout design included grooves to guide the tensioning belts, a tapered internal
19 cap diameter which could work with different drum sizes, and a ball bearing system for smoother tow
20 payout. This system provided stable tension, which allowed for homogenised merging of the two tows
21 on a grooved PTFE roller.

22
23 **3.3. Powder deposition**

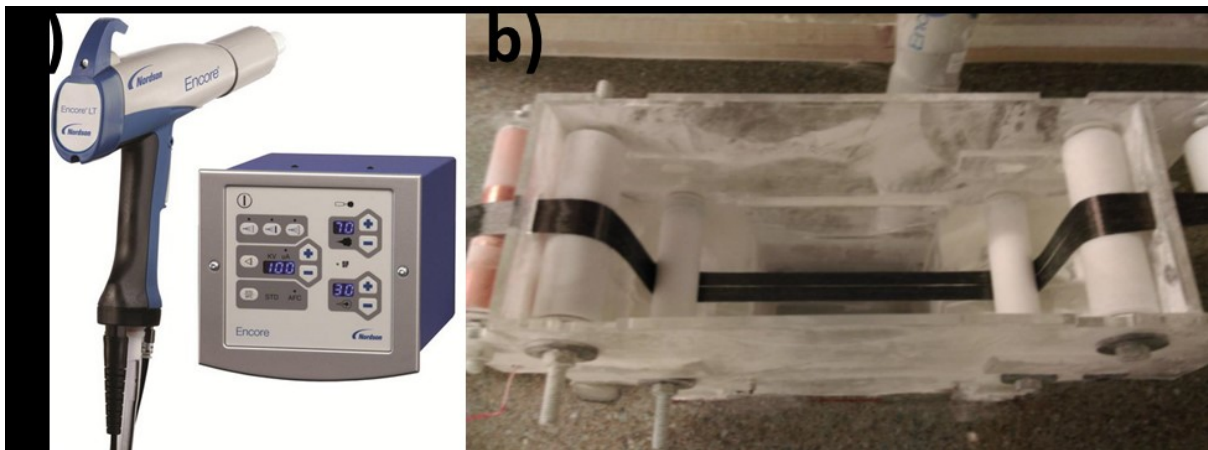
24 There are numerous methods of powder deposition for the towpregging process. Several of these
25 methods were reviewed by Padaki and Drzal [60] including four types of fluidised bed deposition,
26 powder slurry deposition, and electrostatic spraying. Another method is 'powder curtain' deposition
27 which uses an auger to disperse powder across the tow as it passes underneath [44,61]. Early

1 iterations of the pilot towpregging line (presented herein) implemented a form of ‘powder curtain’
2 deposition; using a vibrating hopper and mesh to create the ‘powder curtain’ [62]. This method,
3 however, resulted in inconsistent powder dispersion along the towpreg.

4 For this study, electrostatic spraying was chosen as the method of powder deposition. A 60 W Encore
5 LT electrostatic spray gun, from Nordson, was used to coat the fibres within an enclosed acrylic spray
6 box (Figure 5). The gun was set to 100 kV at 60 μ A, using the smart flow setting for both the air and
7 the powder flows, which helped with adjusting the flow to maintain the same powder velocity. The
8 pressure was set to 5 bar. The surplus powder was evacuated from the spray box using a Nilfisk VHS-
9 110 ATEX extraction unit with High Efficiency Particulate Air HEPA filter (1.1 kW), kept at maximal flow
10 throughout the process to avoid clogging. The powder was recycled to avoid any waste.

11 The electrostatic attraction between the powder-epoxy and the tows was due to the powder being
12 negatively charged by a corona electrode as it passed through the spray gun, while the tows were
13 grounded. This phenomenon has been modelled for towpregging by Woolard and Ramani [63]. They
14 demonstrated that electrostatic spray can coat both sides of the tow due to a ‘wrap-around’ effect,
15 but that the strength of this effect was dependent on the spread tow width. Tow width was constant
16 during this study so as not to introduce variability in powder deposition. This was achieved using
17 grooved rollers at various points in the line.

18



19
20 **Figure 5: a) Encore LT electrostatic spray gun and its control board (© Nordson). b) Plan view of the**
21 **spray box where a cloud of negatively charged powder-epoxy coats the merged tows.**

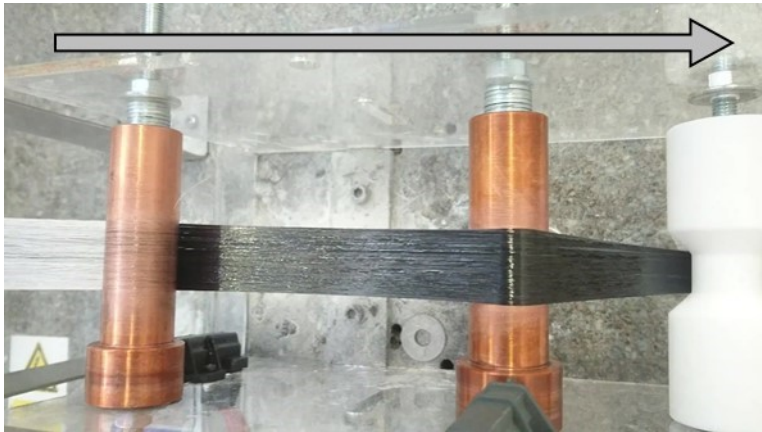
22

23 3.4. Electrical heating of carbon fibre towpreg

24 As carbon fibres are electrically conductive, it has been shown by others that passing a direct current
25 (DC) through the fibres can be used to heat towpreg [41,64] or even cure composite structures [65].
26 This resistive heating is due to the Joule effect, and can achieve rapid increases in temperature while
27 requiring less energy than conventional heating methods [65]. For this reason, resistive heating
28 technology was employed in this study when producing CF towpreg. As shown in Figure 6, two copper
29 rollers were connected to a DC generator using carbon brushes and a differential of 12 volts was set.
30 As the CF passed between the rollers, they closed the circuit and generated heat. The current drawn
31 oscillated between 140 and 160 mA, for a power consumption of only 1.68W to 1.92W. The current
32 fluctuation was due to contact resistances, because of changes in both tow tension and powder
33 concentration during processing.

1
2
3
4
5
6
7
8
9
10

The temperature was monitored with an FLIR TG54 Spot IR Thermometer and was controlled to reach 120°C. The powder in contact with the fibres melted rapidly (Figure 6), demonstrating the ability to work at high speed (up to 15 metres per minute for a 50% fibre volume fraction), while keeping a constant temperature profile between the copper rolls. The copper rollers were coated with a release agent (Frekote 55-NC) and cleaned after each use to avoid any contaminants and inhomogeneity due to excess resin. The first two metres of towpreg were discarded for each run because, at start up, the towpregging line required some time to reach steady state conditions. Removing the first two metres also reduced the risk of any contamination due to Frekote residue.



11
12 *Figure 6: DC electrical heating using copper rollers (plan view). The powder-epoxy coated tows (white) approach the first copper roller on the left. As the tows pass between the rollers, the powder-epoxy melts and sinters onto the carbon fibres (black). The arrow indicates the direction in which the tow is travelling.*

16
17

3.5. Infrared heating for basalt fibre towpreg

18 Due to basalt fibres (BF) being non-conductive, an alternative heat source was required for processing
19 the BF towpreg. From the literature, possible alternatives included tunnel ovens [66–68], convection
20 ovens [41,69,70], hot gas torches [67,69], infrared lamps [61,68,70], and microwave ovens [41]. In this
21 study, the towpregging line used a 1kW infrared (IR) lamp. This lamp had an adjustable power, was 30
22 cm long, and had a reflector to focus radiated heat towards the substrate surface. Again, the
23 temperature was monitored using an IR thermometer throughout the process. To maintain a
24 homogenous heating profile, the maximum line operating speed was set at 5 m/min. The
25 temperatures, however, were initially found to be lower on the non-exposed side. As such, an
26 additional reflective system (a copper sheet) was added to improve the temperature homogeneity on
27 both sides of the BF tow.

28
29

3.6. Cooling and recovery

30 After the powder was melted, the towpreg proceeded to a grooved roller to maintain a constant
31 width. It was then cooled quickly (in about five seconds) by convection and radiation to the
32 surrounding atmosphere, prior to being wound up onto the winding drum. The towpreg temperature,
33 located immediately before the winding drum, was consistently between 30°C and 40 °C, which was

1 lower than the melt temperature of the epoxy. Hence, the towpreg was wound in a vitreous state and
2 maintained optimal straightness due to the tension applied to the fibres throughout the process. The
3 rotating drum itself was powered by a Mellor electric 24 V DC Brushed DC Geared Motor with a
4 maximum output speed of 5.3 rpm. As the drum itself had a diameter of 40 cm, the maximum
5 towpregging process speed was 6.66 m/min. As the processing speed wasn't a constraint in this study,
6 the motor speed was the main parameter used in order to control the fibre volume fraction (FVF) of
7 the towpreg. In this study, all towpreg samples were manufactured using the same powder-epoxy
8 (PE6405).

9

10 4. Composite plate manufacturing and testing

11

12 4.1. Manufacturing overview

13 The overall manufacturing system, illustrated in Figure 7, is described briefly below. Further details
14 are given in subsequent sections.

15 Stages 1 – 2: Towpreg was produced on the towpregging line.

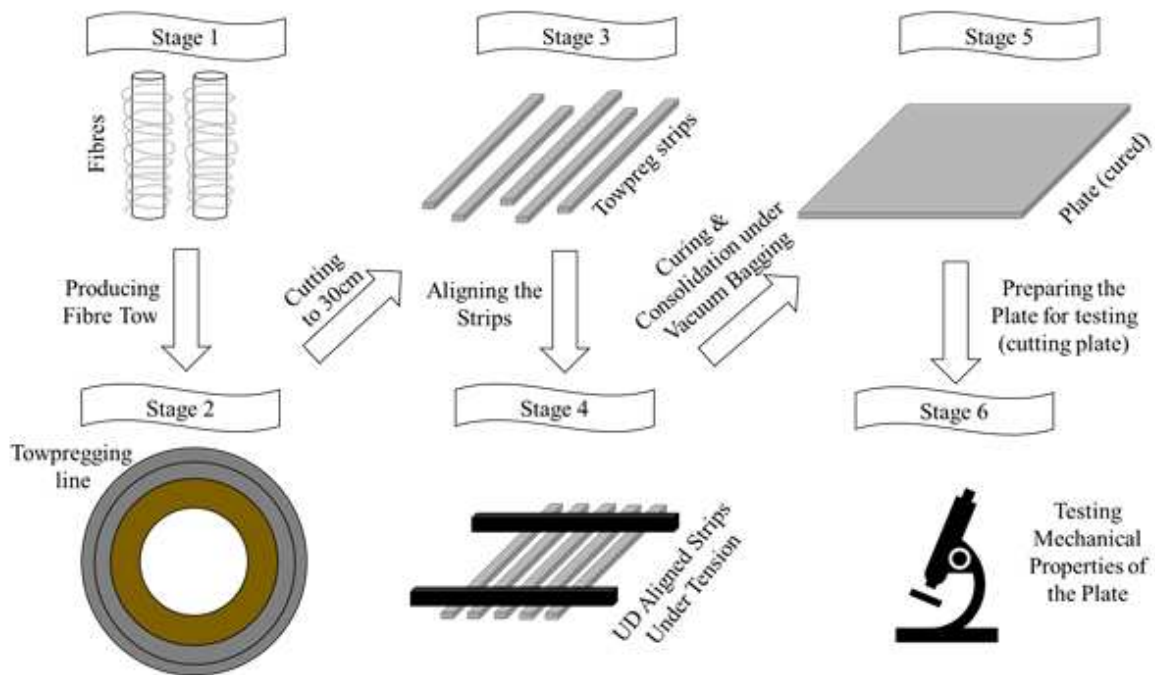
16 Stages 2 – 3: The towpreg was cut into strips of exactly 30 cm length using a guillotine system.

17 Stages 3 – 4: The towpreg strips were aligned and clamped in the fibre tensioning apparatus.
18 This is used to ensure tow straightness in the unidirectional plates during cure.

19 Stages 4 – 5: The tensioned preform was cured under vacuum to produce a unidirectional
20 composite plate.

21 Stages 5 – 6: The composite plate was tabbed and cut, and the resulting specimens were
22 tested and characterised.

23

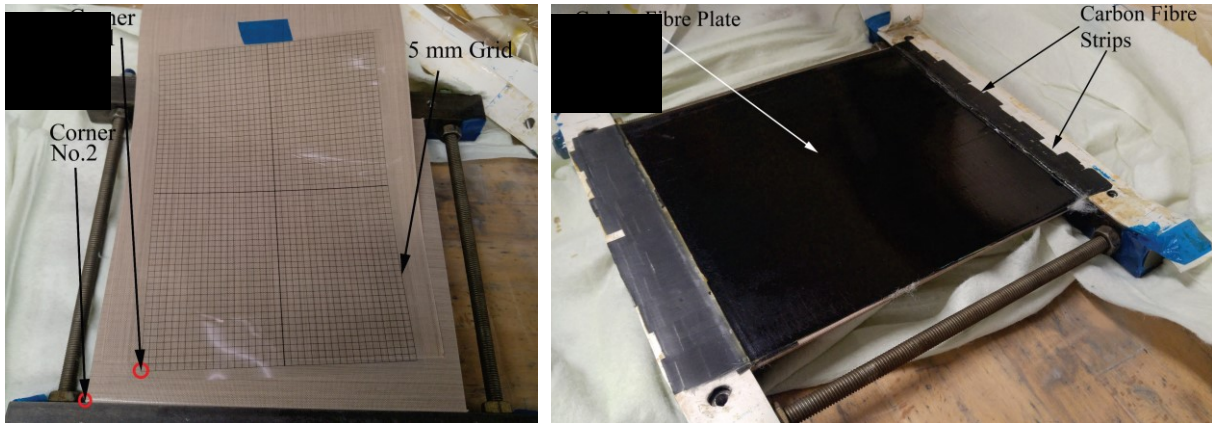


1
2 **Figure 7: Manufacturing overview - from tows to plate manufacturing and testing.**

3
4 **4.2. Plate manufacturing**

5 It has been shown that fibre misalignment and fibre ‘waviness’ can affect the mechanical performance
6 of FRPs [24,71,72]. The results presented by Mamalis et al. [33,35] confirmed that tensioning
7 unidirectional CF/powder-epoxy improved the mechanical properties of the material by increasing the
8 fibre straightness and alignment. Using the towpregging line, highly aligned CF/powder-epoxy may be
9 realised through automation, however, additional handling and processing of tows can lead to
10 increased fibre breakage [43,44]. Therefore, the composite plates for this study were manufactured
11 using the same tow tensioning apparatus developed by Mamalis et al. [33] so that a direct comparison
12 could be made between the two sets of results. By comparing the two, it would be possible to
13 determine if the towpregging process caused any significant fibre damage or breakage.

14 For the plate manufacturing, 30 cm long towpreg ‘strips’ were cut and placed on a PTFE coated flat
15 steel plate; alignment was aided using a plastic grid (see Figure 8a). Once all the strips were placed
16 correctly, they were locked in place by the tensioning apparatus (described further in [33]). Five layers
17 of strips were necessary to obtain 1 mm thick plates. After the alignment grid was removed, a
18 tensioning force of approx. 3.0 kN was applied. This was the force chosen by Mamalis et al. [33], to
19 achieve optimal alignment of the T700S-24K-50C tows. An extra PTFE coated plate was placed on the
20 top of the tensioned towpreg, and the whole tensioning apparatus was then vacuum bagged. The
21 system was kept under vacuum at all times during processing. The curing cycle was set at 40 °C for 12
22 hours to remove all form of moisture from the strips. The temperature then ramped to 130°C for 2
23 hours, melting the powder and consolidating the system. Following this, the plate was cured at 185°C
24 for 2 hours and then cooled to ambient temperature. This methodology was used to produce both
25 UD-CFRP and UD-BFRP plates.



1
2 **Figure 8: Tensioning rig system: a) Strip alignment using a grid, b) Cured plate.**

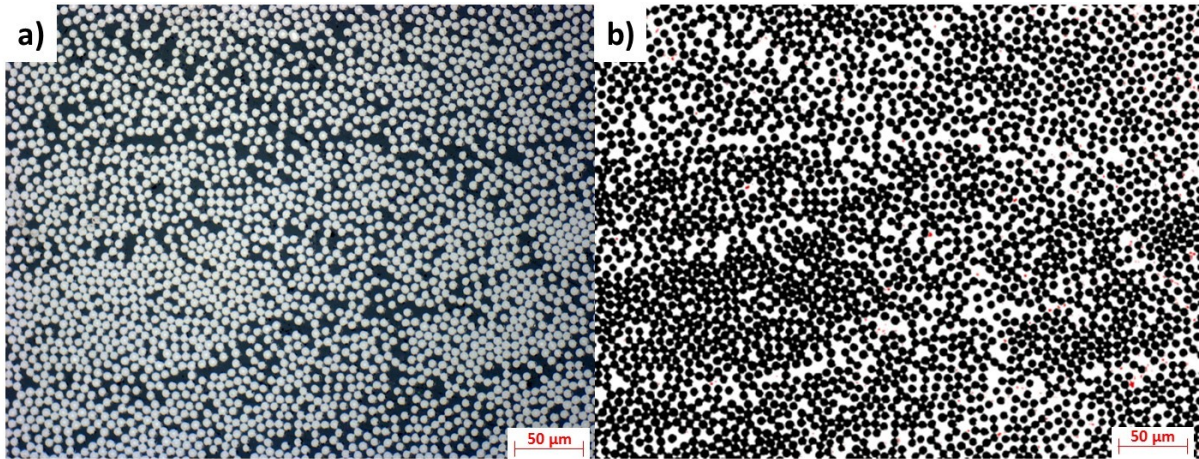
3
4 **4.3. Quality control - weight measurements and void analysis**

5 Fibre volume fraction has an important influence on the mechanical properties of the composite
6 materials. As powder deposition may vary during towpreg production [61], it was important to
7 understand what influence this may have on the mechanical properties of the cured laminates.
8 Different FVF towpreg were produced by slightly modifying the line speed. For each line speed setting,
9 30 cm strips of towpreg were cut and weighed, and the FVF of each strip was determined based on
10 the known volume and mass of the virgin fibre tows. Resin burn-off was also performed on random
11 samples to cross-check their FVF; ASTM D3171-15 – Procedure G – kept at 550°C for 60 min in high
12 temperature furnace.

13 To investigate the influence of FVF over a wide range, the strips were filtered according to four FVF
14 sub-groups: 45% to 50%, 50% to 55%, 55% to 60% and 60% to 65%. A plate for each FVF sub-group
15 was manufactured using the methodology described in the previous section.

16 Optical microscopy was also used in this study. A UD-CFRP specimen was cut into 10 samples and
17 embedded in epoxy. The 10 embedded samples were polished, and their cross sections were observed
18 using an Axioskop® 2MAT optical microscope (Figure 9a). 50 photos (5 per sample) were taken with
19 Axio vision SE64® software, and a FVF analysis was performed on ImageJ®, with 8 bits grayscale
20 settings (Figure 9b). Two filters were used to differentiate the resin, fibres and porosity (fibres contrast
21 threshold: 117 to 255, voids contrast threshold: 0 to 14). The fibre to resin to void surface ratio
22 obtained on each individual photos, combined with a large set of 50 samples, allowed for a FVF
23 estimate. This quantitative method allowed not only to crosscheck the FVF, but also to detect and
24 determine the sample's porosity, as shown in Table 2. The table displays a low porosity (0.437%)
25 compared to other VBO systems and tapes [73]. It is worth noticing that the FVF was found slightly
26 below target (52.07% instead of 52.50%).

27



1
2 **Figure 9: a) Optical microscopy of a powder-epoxy UD-CFRP cross section in reflection mode. b) Resin**
3 **(white), fibres (black), and voids (red) identified using volume fraction analysis with ImageJ software**
4 **filters.**

5
6 **Table 2: Quantitative study of porosity and FVF along a UD-CFRP specimen length, extracted from a**
7 **plate targeting 52.5 % FVF.**

	Porosity (%)	FVF (%)
Mean	0.44	52.07
St. Dev.	0.13	4.03
C.o.V. (%)	29.54	7.74

8
9 **4.4. Mechanical test methodology**

10 The UD-CFRP and UD-BFRP plates were prepared and cut into specimens according to the mechanical
11 test standards used in this study. For UD-CFRP, tensile tests were performed in the longitudinal
12 direction (i.e. 0° direction) according to BS EN ISO 527-5 [74]. 10 specimens were tested for each of
13 the four FVF sub-groups. For UD-BFRP, 0° & 90° tensile tests, 0° & 90° flexural tests, and 0°
14 compression tests were performed according to BS EN ISO 527-5, BS EN ISO 14125 [75], and ASTM
15 D6641/D6641M-16E1 [76], respectively. In each type of test, 8 specimens were tested.

16 Additional 0° tensile tests (BS EN ISO 527-5) were carried out for aged specimens which had been
17 immersed in water. For UD-CFRP, specimens were immersed at room temperature (approx. 21°C),
18 50°C, and 75°C for 100 days. For UD-BFRP (Basaltex only), specimens were immersed at room
19 temperature (approx. 21°C) and 55°C for 60 days. The specimens were periodically weighed using a
20 microbalance to determine the water uptake over the duration of immersion. Tensile tests were also
21 performed periodically to determine the influence of water uptake on the tensile properties of the
22 specimens. In each case, 10 specimens were tested. Tensile testing was carried out when the
23 specimens were still wet.

24 Tensile tests were performed using an MTS Criterion® Model 45 (C45.305) with a 300 kN load cell. A
25 crosshead speed of 2 mm/min was used for all tensile tests. In all tensile test cases, the test specimens
26 were end tabbed with ±45° GRFP and clamped in hydraulic grips with a clamping pressure of approx.
27 100 bar. A speckle pattern was applied to the surface of each specimen and 2D strain was measured
28 with digital image correlation (DIC).

1 Compression tests were performed using an MTS Criterion® Model 45 (C45.305) with a 300 kN load
2 cell and a fixture specially designed by Wyoming Test Fixtures for this specific type of test. Specimens
3 were clamped by applying a torque of 4 N m. A crosshead speed of 1.3 mm/min was used for testing.
4 Again, DIC was used to measure strain for all compression tests.

5 Flexural testing was performed using an Instron 3369 Dual Column Tabletop Test System with a 50 kN
6 load cell. A four point bend fixture was used with an outer span of 45 mm (Class III, Table 4 of BS EN
7 ISO 14125). Testing was carried out with a crosshead speed of 2.15 mm/min. DIC was used to track
8 the midspan deflection of the test specimens.

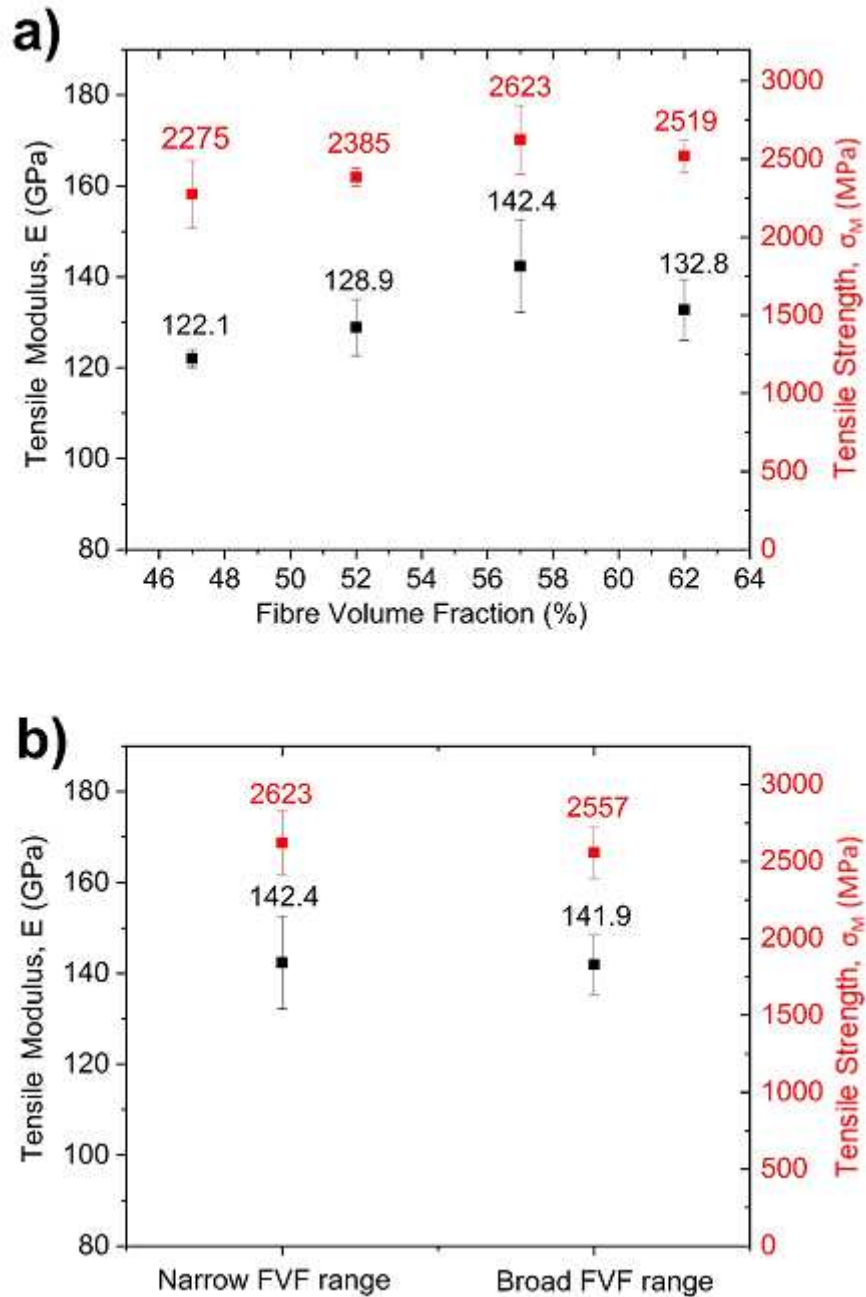
9

10 5. Results and discussion

11

12 5.1. Fibre volume fraction investigations of UD-CFRP

13 Figure 10(a) shows the influence of FVF on the tensile properties of the UD-CFRP. The general trend
14 was that the tensile properties (tensile strength, σ_M , and tensile modulus, E) improved with increasing
15 FVF before decreasing above 57.5%. In addition to the void content analysis presented in Section 4.3,
16 these results suggested that excellent consolidation was achieved at 47.5% FVF and 52.5% FVF. While
17 the mean tensile properties of the 57.5% FVF specimens were the highest of the four sub-groups, the
18 standard deviation (SD) was also the highest for both σ_M and E . This suggested that some specimens
19 were well consolidated while others were not, due to insufficient wet-out and, consequently, poor
20 load transfer between fibres and matrix. At 62.5%, this latter effect worsened and the mean tensile
21 properties decreased. This upper limit in FVF was in agreement with what has been demonstrated for
22 VBO prepreps previously [77]. At higher FVFs, consolidation was limited by the pressure that can be
23 applied i.e. VBO pressure is 1 atm max. In this regard, Gutowski et al. [78] showed that FVF
24 asymptotically approaches a maximum as a fibre bed compresses and resists the applied pressure. In
25 the context of this study, higher FVF could be achieved via pultrusion of the towpreg through a die
26 [69]. Further investigation of this concept was outside the scope of current work, however, it may be
27 explored in future work (see Section 7). Alternatively, it is likely that additional autoclave or heated
28 press processing would be required to achieve better quality and reliability above 60% FVF.



1
 2 **Figure 10: a) Influence of average FVF on 0° UD-CFRP mechanical properties.. b) Influence of strip**
 3 **FVF dispersion at 57.5 % FVF on 0° UD-CFRP mechanical properties.**

4

5 To further study how mechanical properties may be affected by the FVF variation of towpreg, Figure
 6 10(b) shows the results of two sets of specimens (both with an average FVF of 57.5%) which were
 7 manufactured using two different FVF ranges of towpreg. The original plate with 57.5% FVF contained
 8 strips of the same range (55% to 60%), called narrow FVF range. For the second plate, strips of various
 9 FVF were used, altering between high and low FVF layers of strips, but still overall reaching the same
 10 FVF as the first plate (i.e. broad FVF range). The results showed very similar values of σ_M and E . This
 11 suggested that the low viscosity of the powder-epoxy allowed for flow from resin-rich regions to resin-
 12 poor regions, leading to similar homogeneity for the two plates.

1 As previously mentioned, Mamalis et al. have studied the same powder-epoxy system with T700S-
 2 24K-50C fibres [33,35]. In their studies, plates were manufactured in a tensioning apparatus with
 3 powder manually dispersed onto the fibres. By using the same tensioning apparatus in this study, it
 4 was possible to directly compare the 0° tensile properties and determine whether the towpregging
 5 process had any adverse effect on the fibre properties. As shown in Table 3, the 0° tensile strength
 6 (σ_M) for 57.5% FVF specimens was almost identical to that which was reported by Mamalis et al. (for
 7 59% FVF), while the 0° tensile modulus (E) was slightly higher. This confirms that the towpregging line
 8 does not have any significant adverse effect on the CF, such as fibre breakage.

9 Table 3 also shows the 0° tensile properties of other equivalent material systems of interest. As can
 10 be seen, the 57.5% FVF specimens were stronger and stiffer than the data reported by Toray for UD
 11 epoxy composites reinforced with T700s carbon fibres [56] while having a slightly lower FVF (57.5%
 12 compared to Toray's 60%). Comparatively, normalised data shows a substantial increase in both
 13 strength (+7.33%) and stiffness (+10.06%). This improvement was attributed to the improved fibre
 14 alignment achieved with the tensioning apparatus. This highlighted the technological potential for
 15 industrial manufacturing processes where carbon fibres are kept under tension, such as pultrusion,
 16 filament winding, and, to a lesser extent, ATP. For further comparison, Table 3 includes the 0° tensile
 17 properties of two flat-section pultruded CF/epoxy systems, both used for manufacturing turbine blade
 18 spars [79,80]. Both pultruded systems show higher FVF, but only the tensile modulus of Röchling EP-
 19 CFK (66% FVF) is higher than the 57.5% FVF UD-CFRP produced in this study. The lower 0° tensile
 20 strength can be attributed to a difference in fibre type and fibre quality e.g. the individual tensile fibre
 21 strength of T700S fibres [56] are markedly higher than Zoltek's PX35 fibres [81].

22
 23
 24

Table 3: Comparison of the 0° tensile properties for powder-epoxy UD-CFRP and equivalent material systems of interest.

	FVF (%)	σ_M (MPa)	SD (MPa)	E (GPa)	SD (GPa)
Towpreg line	47.5	2275.0	212.3	122.1	1.9
	52.5	2385.0	56.5	128.9	6.1
	57.5	2623.0	220.8	142.4	10.2
	62.5	2519.0	106.7	132.8	6.7
Mamalis et al. [33]	59.2	2650	-	134	-
Toray T700S [56]	60	2550	-	135	-
Gurit CF SparPreg [82]	56*	2234	-	140	-
Zoltek PX35 Pultruded Plate [83]	62	2350	-	140	-
Röchling EP-CFK [79]	66	2000	-	150	-

25 * Normalised to 56% in the technical data sheet

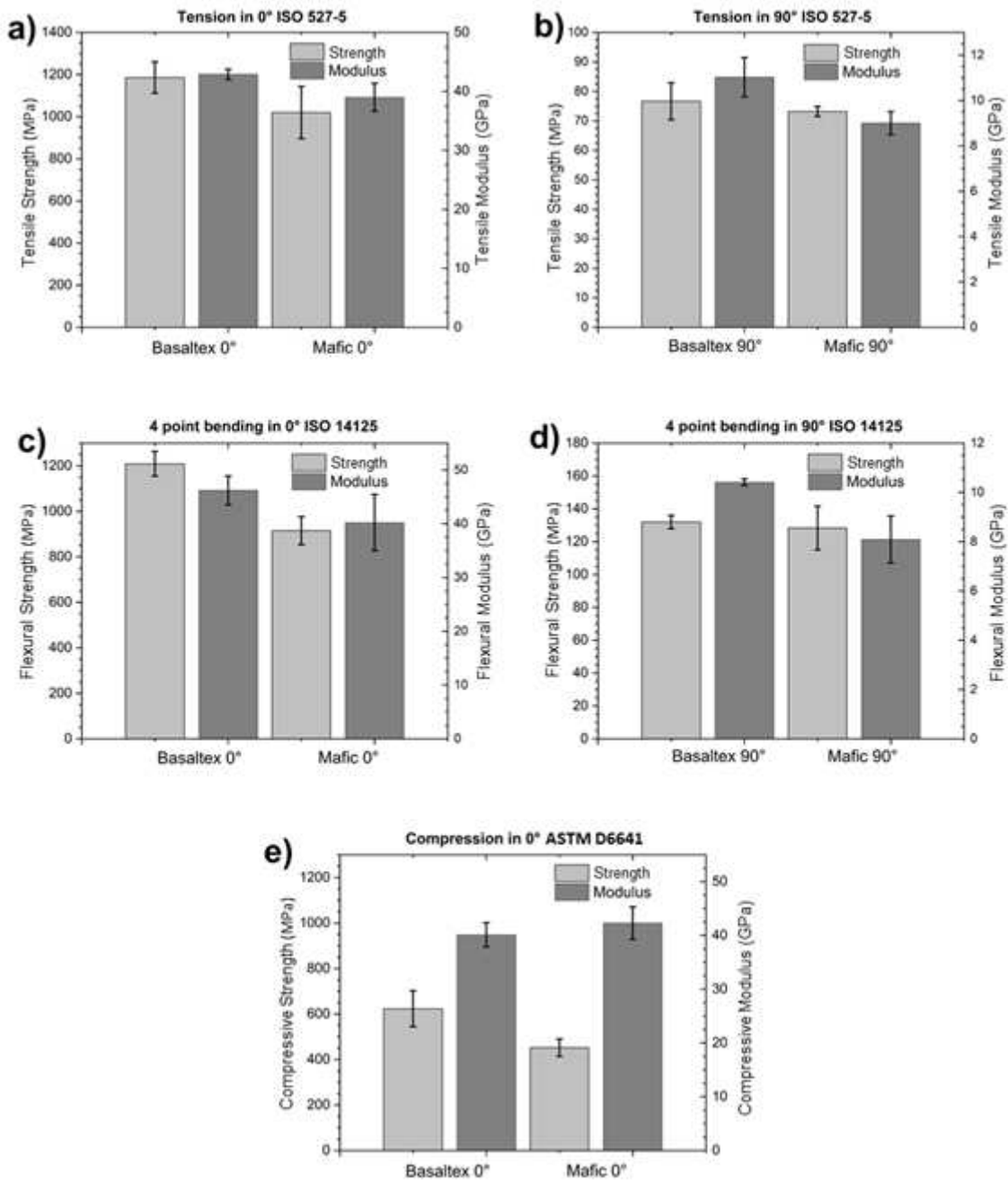
26

27 5.2. Comparison of UD-BFRP plates

28 Powder-based UD-BFRP plates were manufactured to compare Mafic and Basaltex basalt fibres. A FVF
 29 of 50% was targeted to ensure that homogeneous samples were processed. The results of the various

1 tests are plotted in Figure 11. Overall, the Basaltex fibre composites exhibited better mechanical
 2 properties than those with Mafic fibres. The mean strength of the Basaltex composite specimens was
 3 superior in 0° tension (+14%), 0° flexure (+24.3%) and 0° compression (27.4%), when compared to the
 4 Mafic composites. Basaltex composite specimens were also stiffer in 0° tension (+9.1%) and 0° flexure
 5 (+12.9%) but not in 0° compression (-5.5%). This important mismatch in properties is not unexpected
 6 as the basalt fibres are naturally sourced, and will display different properties as their chemical
 7 compositions depends on their extraction location [11].

8



9

10 **Figure 11: Mechanical properties of Basaltex and Mafic basalt towpreg based composites in tension**
 11 **(a & b), flexure (c & d) and compression (e).**

12

1 The mechanical properties in the transverse direction allow a direct comparison of the interfacial
 2 properties, as the powder-epoxy is the same in both cases. Basaltex and Mafic BFRP displayed very
 3 similar strength in both 90° tension (+4.6% for Basaltex) and 90° flexure (+3% for Basaltex)
 4 configurations. As the tensile strength in transverse direction is largely matrix and fibre interface
 5 dominated, it was not surprising to obtain similar properties. Basaltex samples still exhibited much
 6 better transverse stiffness properties than Mafic specimens, doubling the difference already obtained
 7 longitudinally. It is likely that this is a result of a more effective fibre sizing.

8 For further comparative purposes, the results are reproduced in Table 4, Table 5, and Table 6 alongside
 9 mechanical properties for similar material systems. Direct comparison with other BFRP studies is
 10 difficult because much of the existing literature has focussed on the mechanical properties of bi-
 11 directional or multi-directional laminates [11,12]. Wang et al. [84] studied mechanical properties of
 12 UD-BFRP (epoxy matrix) in the 0° direction, comparing it to UD-GFRP in tension, compression, and
 13 flexure. They reported that the 0° tensile strength of the UD-BFRP (640 MPa) was much lower than
 14 UD-GFRP (1029 MPa), and attributed this to a variation in the tensile strength of individual fibre
 15 strands i.e. large variation in basalt fibre quality. Table 4 confirms that their values were much lower
 16 than the tensile strengths reported herein for Mafic fibres (37% lower) and Basaltex fibres (46%
 17 lower). Nevertheless, their 0° flexural strength was similar to the values for Mafic and Basaltex fibres,
 18 and notably, their 0° compressive strength was higher in both cases.

19

20 **Table 4: Comparison of the tensile properties for powder-epoxy UD-BFRP and equivalent material**
 21 **systems of interest.**

	FVF (%)	Test direction	σ_M (MPa)	SD (MPa)	E (GPa)	SD (GPa)
Mafic towpreg	50	0°	1020.0	124.0	39.0	2.4
		90°	73.2	1.7	9.0	0.5
Basaltex towpreg	50	0°	1186.0	74.3	42.9	0.9
		90°	76.7	6.3	11.0	0.9
Wang et al. [84] (UD-BFRP)	-	0°	640	-	40.8	-
Gurit GF	56**	0°	1225	-	48	-
Sparpreg* [82]	50	90°	42	-	12	-
Röchling EP-GZUV [79]	64	0°	1500	-	45-50	-

22 * Values for 1600 g/m²

23 ** Normalised to 56% in TDS

24

25 Davies and Verbouwe [15] investigated the mechanical properties of a stitched BFRP fabric with 357
 26 g/m² in the 0° direction and 50 g/m² in the 90° direction (ratio of 7:1). Their quasi-UD BFRP fabric was
 27 made using Basaltex fibres sized for epoxy with alkosilane agent, which are believed to be very similar
 28 to the Basaltex fibres used in this study. The flexural strength reported in their work was 698 MPa,
 29 which is 42.3% lower than the value obtained in this study. Likely, this was due to the presence of

1 fibres in the transverse direction; typically used to stabilise the fabric while being laid up. Having less
 2 fibres aligned with the loading direction will reduce the strength in that direction, and will also
 3 increase the crimp of the BFRP, thus reducing the ultimate strength of composite materials [85].

4 Table 4, Table 5, and Table 6 also display values for commercially available material systems that are
 5 used for turbine blade spar caps; Gurit GF Sparpreg [82], a UD-GFRP prepreg system, and Röchling EP-
 6 GZUV [79], a UV-cured GF/epoxy pultruded section. Both UD-BFRP systems from this study compare
 7 favourably with the 0° tensile properties of the commercially available UD-GFRP (when factoring in
 8 the higher FVFs reported for the latter). Notably, the 90° tensile strengths were markedly higher for
 9 the powder-epoxy systems than for Gurit GF Sparpreg. These values were equal to the tensile strength
 10 of the neat powder-epoxy matrix (73.1 MPa [35]), which was atypical for conventional epoxy systems.
 11 Often some strength reductions are expected for transverse UD composite properties compared to
 12 neat matrix properties. These reductions are usually attributed to the presence of defects (such as
 13 voids), which form during composite processing, and aid crack initiation and propagation through the
 14 resin matrix. This is a particular issue for conventional epoxies, which are brittle, however, toughened
 15 epoxy systems have reported significantly better 90° tensile strengths: 90 MPa for Solvay’s CYCOM®
 16 5276-1 (G40-800 Tape) [86], 77 MPa for Hexcel’s Hexply® 8552 UD CF prepreg [87], and 64 MPa for
 17 Hexcel’s Hexply® M73/IM7 UD tape. In the latter case, the 90° tensile strength of the composite
 18 approached the tensile strength of the neat M73 epoxy i.e. 77 MPa). The improved performance of
 19 toughened epoxies may be attributed to their greater ability to resist crack growth compared to
 20 conventional systems. For the powder-epoxy in this study, it has been shown to have relatively ductile
 21 behaviour with exceptionally high mode I fracture toughness; between 1,100 and 1,900 J/m²,
 22 depending on the fibre and sizing [35,88]. It should be noted that the ductile behaviour of the powder-
 23 epoxy is also evident in the tensile failure strain values for the 90° specimens: 0.92 ± 0.14%, which is
 24 high, compared to standard epoxy UD materials.

25
 26 **Table 5: Comparison of the flexural properties for powder-epoxy UD-BFRP and equivalent material**
 27 **systems of interest.**

	FVF (%)	Test direction	σ_M (MPa)	SD (MPa)	E (GPa)	SD (GPa)
Mafic towpreg	50	0°	915.0	61.3	40.2	5.2
		90°	128.0	13.3	8.1	0.9
Basaltex towpreg	50	0°	1209.0	54.3	46.2	2.7
		90°	132.0	4.0	10.4	0.1
Wang et al. [84] (UD-BFRP)	-	0°	1115	-	43.7	-
Gurit GF Sparpreg* [82]	50	0°	1347	-	42	-
Röchling EP-GZUV [79]	64	0°	890-1020	-	35-45	-

28 * Values for 1200 g/m²

29

1 The strong transverse performance of the UD-BFRP was confirmed by the 90° flexural properties which
 2 were similar to those reported by Mamalis et al. [33] for powder-epoxy UD-CFRP. 0° flexural properties
 3 were also similar to the UD-GFRP systems shown in Table 5. For 0° compressive properties (Table 5),
 4 however, the UD-BFRP again performed poorly compared to UD-GFRP. Failure was predominantly due
 5 to kinking of the fibres, despite the high degree of fibre alignment, which suggests that the ductile
 6 nature of the powder-epoxy played a role in the comparatively low 0° compressive properties.

7

8 **Table 6: Comparison of the compressive properties for powder-epoxy UD-BFRP and equivalent**
 9 **material systems of interest.**

	FVF (%)	Test direction	σ_M (MPa)	SD (MPa)	E (GPa)	SD (GPa)
Mafic towpreg	50	0°	452.0	38.0	42.3	3.0
Basaltex towpreg	50	0°	623.0	78.9	40.1	2.2
Wang et al. [84]	-	0°	836	-	-	-
Gurit GF Sparpreg* [82]	56**	0°	950	-	47	-

10 * Values for 1600 g/m²

11 ** Normalised to 56% in TDS

12

13 5.3. Hygrothermal aging

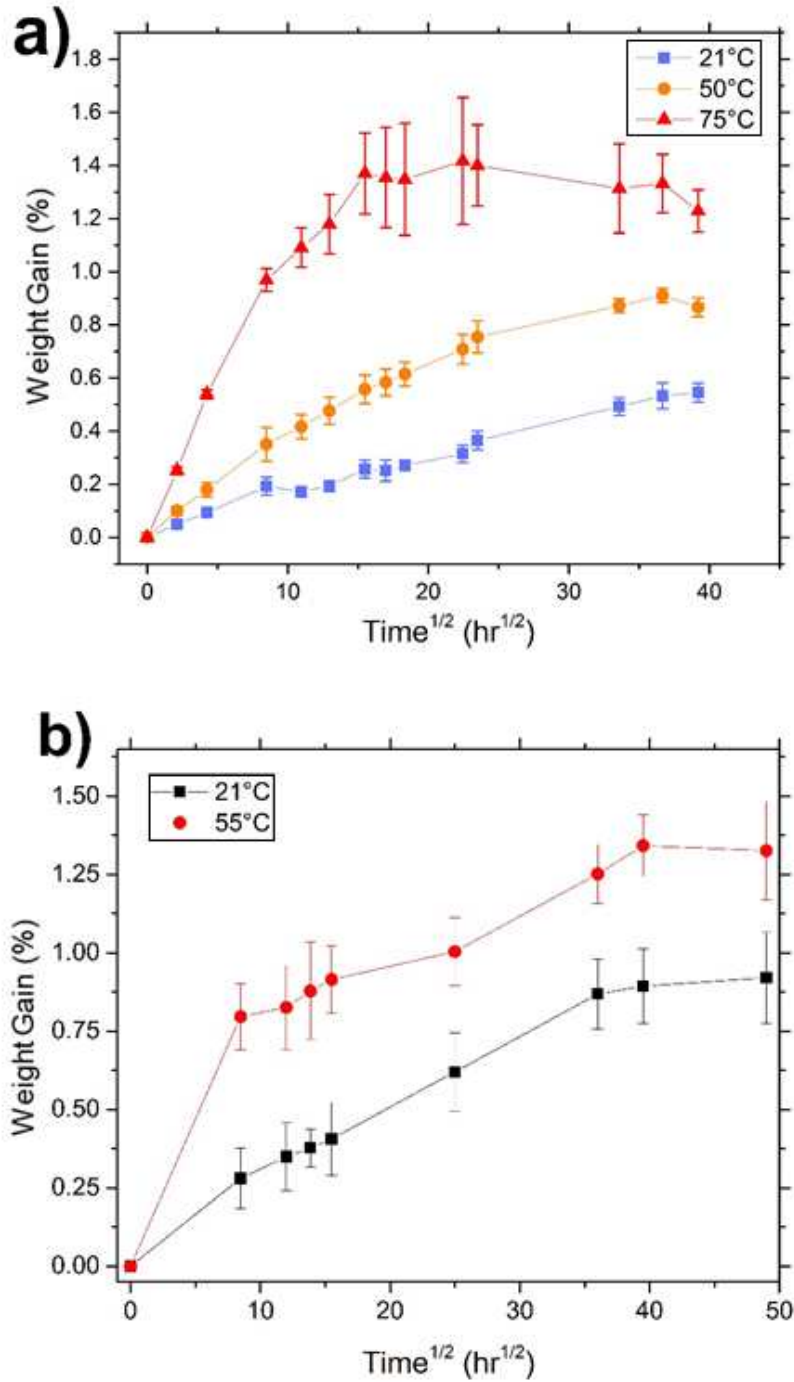
14 The results for 0° tensile testing of UD-CFRP (Figure 10 (a) and Table 3) show that the standard
 15 deviation was the lowest at 52.5% FVF; highlighting better reproducibility. As such, this FVF range was
 16 selected for a subsequent hygrothermal ageing study. In addition, Basaltex UD-BFRP was selected for
 17 the hygrothermal ageing study as it displayed better mechanical properties than Mafic UD-BFRP. UD-
 18 CFRP and UD-BFRP specimens were immersed in water as described in Section 4.4. In both cases, the
 19 temperature had an influence on the absorption rate and the water saturation level (see Figure 12).

20 As expected, rates of water absorption were highly temperature dependent. In the case of UD-CFRP,
 21 the specimens reached saturation within approx. 15 days of immersion at 75°C, but showed a high
 22 degree of scatter after that point with a potential loss of mass. Such a phenomena is not uncommon
 23 due to leaching of soluble components of the polymer matrix, which is exacerbated at higher
 24 temperatures [36]. At lower immersion temperatures, the UD-CFRP and UD-BFRP displayed similar
 25 characteristics, but differed in the quantity of water absorbed. Grogan et al. [36] reported similar
 26 differences in weight gain for powder-epoxy CFRP and GFRP specimens, despite the specimens having
 27 similar FVFs. Assuming that the water was predominantly absorbed by the resin matrix, they
 28 attributed this discrepancy to the difference in resin mass fraction (i.e. the resin mass fraction in the
 29 GFRP was lower due to the higher density of glass fibres (approx. 2520 kg/m³) compared to carbon
 30 fibres (approx. 1800 kg/m³)). They stopped short, however, of calculating the weight gain with respect
 31 to the resin mass fraction, W_r , using the simple equation,

$$W_r = \frac{W_c}{m_r} \quad (1)$$

1 Where W_c is the weight gain of the composite material, and m_r is the resin mass fraction of the
 2 composite material.

3



4
 5 *Figure 12: Composite weight gain (W_c) due to immersion of powder-epoxy based UD-CFRP (a) and*
 6 *UD-BFRP (b) against the square root of time at different temperatures.*

7

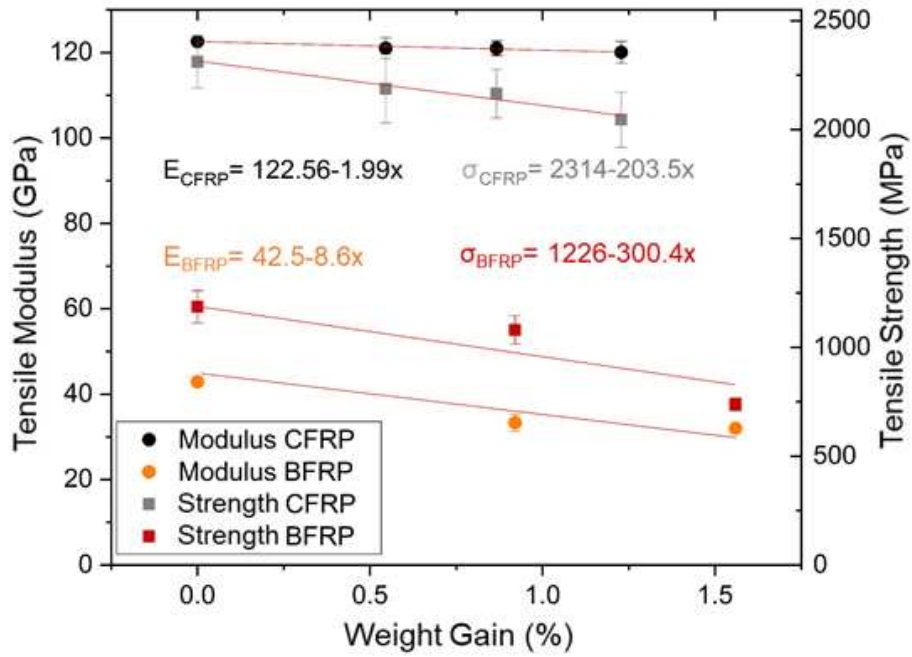
1 Using Equation 1, it is possible to quantify the weight gain with respect to the resin mass fraction and
2 compare it to the equivalent value for neat resin. For example, after 60 days at 50°C and ambient
3 pressure, Grogan et al. [36] reported a weight gain of approx. 0.8% for GFRP (reported resin mass
4 fraction of 33%), and approx. 1.0% for CFRP (reported resin mass fraction of 42%). Using Equation 1,
5 this equates to 2.42% weight gain w.r.t to the resin mass fraction of the GFRP, and 2.38% weight gain
6 w.r.t to the resin mass fraction of the CFRP. In comparison, under the same immersed conditions, they
7 reported that the neat epoxy powder (density of 1220 kg/m³) had a weight gain of approx. 2% with
8 respect to its initial weight. This shows that both composites absorbed similar quantities of water, and
9 both were slightly higher values than the weight gain of the neat resin. Applying the same calculation
10 to the UD-CFRP in the current study (resin mass fraction of 38%), after 60 days at 50°C and ambient
11 pressure, the specimens had a weight gain of approx. 2.26% w.r.t to the resin mass fraction of the
12 CFRP. This shows excellent consistency between the two studies, and offers a simple, yet powerful
13 method for analysing the influence of the polymer matrix on water absorption.

14 Although immersed ageing of the UD-BFRP was carried out at 55°C, it was considered that Equation 1
15 could provide some indication of how the composite performs in comparison to the UD-CFRP. As such,
16 after 60 days at 55°C and ambient pressure, the UD-BFRP specimens were calculated to have increased
17 in weight by approx. 4.14% with respect to the resin mass fraction (31.4% for a fibre density of 2670
18 kg/m³ [58]). This was double the weight absorbed by the UD-CFRP in the same time span, but was
19 consistent with the values reported by Davies and Verboouwe [15]. They performed water immersion
20 studies (at 4°C, 25°C, 40°C, and 60°C) on quasi-UD GF/epoxy and BF/epoxy; Basaltex fibres were used
21 in the latter case also. Interpolating between 40°C and 60°C at 60 days, their GFRP exhibited a weight
22 gain of approx. 0.95%, while their BFRP exhibited a weight gain of approx. 1.15%. For their reported
23 resin mass fractions of 36.2% (GFRP) and 33.5% (BFRP), this equates to weight gains, with respect to
24 resin mass fraction, of 2.62% and 3.43%. Despite potential errors introduced by interpolation and
25 approximation, these values are relatively consistent with both the values in this study (for BFRP) and
26 the study by Grogan et al. [36] (for GFRP). For these studies, at least, this would suggest that water
27 absorption in CFRP and GFRP was predominantly via the resin matrix, while there is some additional
28 water absorption mechanism for the BFRP. As it is expected that the fibres would not absorb a
29 significant amount of water (, this additional mechanism may be due to capillary action at the fibre-
30 matrix interface, which can be damaged by swelling of the matrix [7]. Higher temperatures exacerbate
31 this behaviour, which would allow more water ingress and increased saturation levels.

32 |The effect of the additional water absorption was clearly visible in the aged mechanical performance
33 of the UD-CFRP and UD-BFRP, as shown in Figure 13, which shows the 0° tensile strength and modulus
34 plotted in relation to their weight gain due to water absorption. Based on the linear fits presented in
35 Figure 13, UD-CFRP showed a reduction of 1.62% in tensile modulus and 8.79% tensile strength per 1
36 % weight gain, whereas basalt fibre samples displayed a greater dependency on water ingress, with
37 reductions of 20.2% in tensile modulus and 24.5% in tensile strength per 1 % weight gain. Note that
38 the individual data points are given in Table 7 and Table 8.

39 Davies and Verboouwe [15] tested their aged specimens in quasi-static flexure and cyclic flexure. The
40 quasi-static tests, relevant to this study, showed comparatively less influence of water ageing on
41 flexural modulus (approx. 5% reduction), but a very similar influence on flexural strength (approx.
42 24.6% reduction). They also noted that their GFRP were less sensitive to water ageing.

43 The increased water ageing of the BFRP was most likely coupled to the increased water absorption,
44 and was also likely a result of damage accumulating at the fibre-matrix interface. This suggests that
45 improved fibre sizings must be developed for BFRP to better retain its mechanical properties in
46 immersed conditions.



1
2 **Figure 13: Mechanical properties of powder-epoxy based UD-CFRP and UD-BFRP in relation to their**
3 **composite weight gain (W_c) due to water absorption.**

4

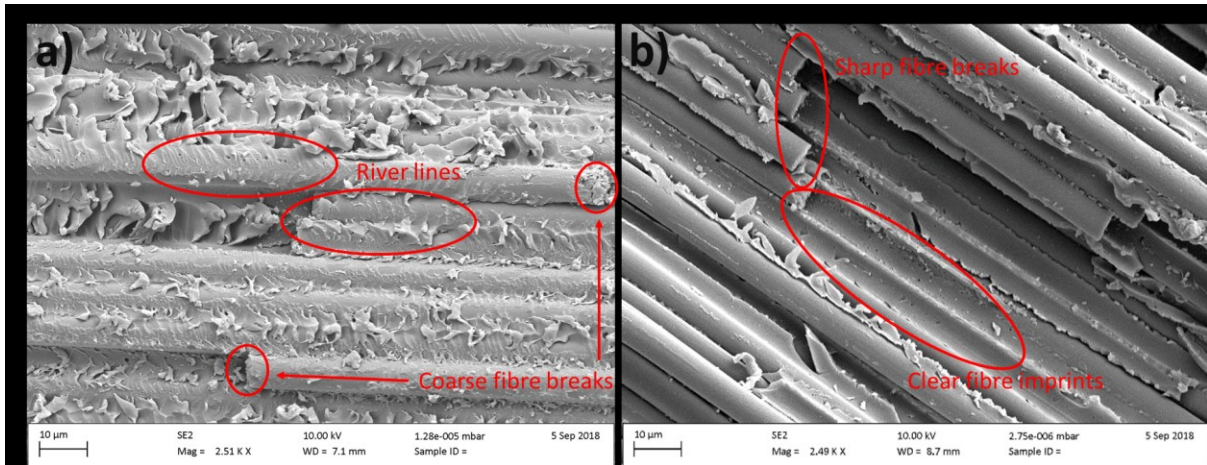
5 **Table 7: The influence of water ageing on the 0° tensile properties of UD-CFRP.**

W_c (%)	σ_M (MPa)	SD (MPa)	E (GPa)	SD (GPa)
0.00	2311	120.2	122.6	0.5
0.55	2187	157.1	121.0	2.4
0.87	2164	112.1	121.0	1.7
1.23	2045	128.0	120.8	2.5

6

7 **Table 8: The influence of water ageing on the 0° tensile properties of UD-BFRP.**

W_c (%)	σ_M (MPa)	SD (MPa)	E (GPa)	SD (GPa)
0.00	1186	74.3	42.9	0.9
0.92	1080	64.9	33.3	2.0
1.56	737	29.9	32.0	0.5



1
2 **Figure 14: SEM fractographic photos of UD-CFRP epoxy samples a) dry and b) hygrothermally aged**
3 **at 21°C for 1600 hours.**

4 The fracture comparison between dry and hygrothermally aged (21°C) UD-CFRP samples highlights
5 two different failure mechanism. The dry sample fracture reveals coarse fibre fractures with multiple
6 fragmentation. One can also observe the presence of river lines on both the fibres and the fibre
7 imprints. This fracture behavior is typical of good fibre/matrix interface cohesion, leading to a brittle
8 and explosive failure. The presence of water in Figure 14(b) discloses a very different fracture
9 behavior. Sharp, clean fibre breaks and clear fibre imprints are witness to a poorer energy transfer at
10 the interface during breakage, when compared to the dry case of Figure 14 (a). The presence of water,
11 plasticizing and swelling the resin, likely caused a poorer interfacial cohesion which resulted in a more
12 ductile and progressive failure.

13
14 **6. Conclusions**

15 This study investigated a novel powder-epoxy towpregging line for manufacturing unidirectional
16 carbon fibre reinforced polymers (UD-CFRP) and unidirectional basalt fibre reinforced polymers (UD-
17 BFRP) as alternative material systems for ocean energy sub-structures such as wind and tidal turbine
18 blade spars. One type of carbon fibre (CF) towpreg and two types of basalt fibre (BF) towpregs were
19 produced; with powder-epoxy being used as the resin matrix in all cases.

20 Due to the processing characteristics of the powder-epoxy, it was possible to manufacture towpreg at
21 120°C without inducing any significant curing. Furthermore, once cooled below approx. 40°C (i.e. its
22 glass transition temperature), it was possible to store the towpreg under ambient conditions with no
23 risk of out-time effects.

24 Electrical joule heating was used during towpregging to sinter/melt the powder-epoxy onto the carbon
25 fibres, while IR heating was used for basalt fibres. Both heating methods were successful in producing
26 towpreg, however, it was found that electrical heating of CF towpreg resulted in a more homogeneous
27 heating profile.

28 Electrostatic spraying was found to be an efficient method of powder deposition, however, a
29 consistent deposition rate and stable line tension were found to be important for maintaining a
30 uniform towpreg fibre volume fraction (FVF). Tensile tests (0° direction) on UD-CFRP specimens
31 showed that strength and modulus increased with FVF up to 57.5%, but then reduced due to
32 insufficient laminate processing pressure (i.e. vacuum-bag-only), resulting in poor consolidation at
33 higher FVFs. It was also shown that the FVF range of CF/powder-epoxy towpreg had a negligible effect

1 on the 0° tensile properties as long as the mean FVF was at the required level. This was attributed to
2 the low viscosity of the powder-epoxy, which allowed it to flow from resin-rich regions to resin-poor
3 regions.

4 In all cases, test laminates were manufactured with a fibre tensioning apparatus, which improved fibre
5 alignment and straightness, thereby improving the mechanical properties of the unidirectional
6 composite laminates. By comparing directly to the literature, it was possible to show that the
7 towpregging process had no adverse effect on the 0° tensile properties of the composite. Moreover,
8 comparison with commercially available UD-CFRP material systems showed that similar or better 0°
9 tensile properties were achievable with the CF towpreg.

10 For the two types of basalt fibre investigated, UD-BFRP manufactured with Basaltex fibres generally
11 outperformed UD-BFRP manufactured with Mafic fibres in a series of mechanical tests; 0° & 90°
12 tension, 0° & 90° flexure, and 0° compression. This confirmed that there was some variation between
13 basalt fibre suppliers, however, similar variations might be expected between glass fibre suppliers or
14 carbon fibre suppliers (e.g. Toray T700S compared to Zoltek PX35). Comparing to UD-BFRP from the
15 literature and commercially available UD-GFRP, the two sets of UD-BFRP performed well in tension
16 and flexure, with notably high 90° properties similar to the properties of the neat powder-epoxy.
17 Despite this, both sets underperformed in 0° compression tests. The high 90° properties and low 0°
18 compression properties are thought to be related to the ductility and toughness of the powder-epoxy.

19 Finally, a hygrothermal ageing study of UD-CFRP (52.5% FVF) and UD-BFRP (Basaltex, 50% FVF) showed
20 that both composites absorbed water and aged as a result. For UD-CFRP, the weight gain (w.r.t to
21 resin mass fraction) due to water uptake was similar to the literature for neat powder-epoxy. For UD-
22 BFRP, however, the weight gain almost doubled (with respect to resin mass fraction) for similar ageing
23 conditions to the CFRP. Further analysis of values reported in the literature, confirmed this trend for
24 UD-CFRP and UD-BFRP. This suggested that there was some additional mechanism for water uptake
25 in the UD-BFRP specimens other than absorption into the resin matrix; potentially capillary action due
26 to damage at the fibre-matrix interface. This hypothesis was supported by a greater reduction in 0°
27 tensile properties for UD-BFRP than UD-CFRP after immersed ageing. Similar trends were noted in the
28 literature for UD-GFRP and UD-BFRP.

29 Overall, this study showed that the pilot towpregging line has potential for upscaling to produce UD
30 materials for the ocean energy industry. In particular, the UD-CFRP produced in this study performed
31 well against commercially available material systems and in immersed conditions. The results for UD-
32 BFRP show an increasing potential for commercial use, but further development is still required to
33 compete with GFRP or CFRP, particularly in area of immersed performance.

34

35 7. Future work

36 This study covered a broad range of themes; from material development and production, to
37 mechanical testing and hygrothermal ageing. As such, exploring many aspects in detail were outside
38 the current scope of work. Nevertheless, the results of the study open numerous possibilities for
39 future work, some of which are presented here.

40 Firstly, this technology requires further automation before reaching an acceptable industrial level of
41 reliability. Better process control and a deeper understanding of how each process parameter
42 influences towpreg production can be achieved via process monitoring and process modelling. In this
43 regard, key processes are tow tensioning, electrostatic deposition, heating, and consolidation. With

1 further development, data from tension meters, IR sensors, solid particle concentration sensors, and
2 optical sensors could be logged in real time, and combined with process modelling to form a closed
3 loop system which can be optimised and self-regulate.

4 The ability to produce high quality powder-epoxy towpreg would open numerous possibilities in terms
5 of application due to its latent curing characteristics. Future projects will consider application of the
6 towpreg in subsequent manufacturing processes. Towpreg could be used 'as-is' for filament winding,
7 subsequently reprocessed into tape for ATP, or pultruded into net sections which can later be
8 reformed. This latter example is significant in the context of the current work, which is aimed at
9 developing alternative, low-cost materials for wind and tidal energy.

10

11 Acknowledgements

12 The authors would like to thank the European Commission for the financial support of the
13 MARINCOMP and POWDERBLADE projects (FP7 IAPP ID: 612531 and Horizon 2020 ID: 730747
14 respectively), which made this study possible. The authors would also like to thank industrial
15 supporters Freilacke, Mafic, Basaltex and Toray for supplying the material and details required for this
16 study.

17

18 References

- 19 [1] International Energy Agency. Data and statistics 2020. [https://www.iea.org/data-and-](https://www.iea.org/data-and-statistics?country=WORLD&fuel=Energy%20supply&indicator=Electricity%20generation%20by%20source)
20 [statistics?country=WORLD&fuel=Energy supply&indicator=Electricity generation by source](https://www.iea.org/data-and-statistics?country=WORLD&fuel=Energy supply&indicator=Electricity generation by source)
21 (accessed June 1, 2020).
- 22 [2] WWEA. Wind Power Capacity reaches 546 GW, 60 GW added in 2017 2018.
23 <https://wwindea.org/blog/2018/02/12/2017-statistics/> (accessed June 1, 2020).
- 24 [3] Segura E, Morales R, Somolinos JA, López A. Techno-economic challenges of tidal energy
25 conversion systems: Current status and trends. *Renew Sustain Energy Rev* 2017;77:536–50.
26 <https://doi.org/10.1016/j.rser.2017.04.054>.
- 27 [4] Hollaway LC. 10 – High performance fibre-reinforced composites for sustainable energy
28 applications. *High Perform. Text. their Appl.*, Woodhead Publishing; 2014, p. 366–417.
29 <https://doi.org/https://doi.org/10.1533/9780857099075.366>.
- 30 [5] Harper P, Hallett S, Fleming A, Dawson M. 9 – Advanced fibre-reinforced composites for
31 marine renewable energy devices. *Mar. Appl. Adv. Fibre-Reinforced Compos.*, Woodhead
32 Publishing; 2016, p. 217–32. [https://doi.org/https://doi.org/10.1016/B978-1-78242-250-](https://doi.org/https://doi.org/10.1016/B978-1-78242-250-1.00009-0)
33 [1.00009-0](https://doi.org/https://doi.org/10.1016/B978-1-78242-250-1.00009-0).
- 34 [6] Nijssen R, de Winkel GD. 5 - Developments in materials for offshore wind turbine blades.
35 *Offshore Wind Farms*, Woodhead Publishing; 2016, p. 85–104.
36 <https://doi.org/https://doi.org/10.1016/B978-0-08-100779-2.00005-2>.
- 37 [7] Davies P, Rajapakse YDS. *Durability of Composites in a Marine Environment*. 1st ed. Springer
38 Netherlands; 2014. <https://doi.org/https://doi.org/10.1007/978-94-007-7417-9>.
- 39 [8] Davies P, Rajapakse YDS. *Durability of Composites in a Marine Environment* 2. 2018.
40 https://doi.org/10.1007/978-3-319-65145-3_13.
- 41 [9] Ross A. Basalt Fibers: Alternative to Glass ? *Compos World* 2006.

- 1 <https://www.compositesworld.com/articles/basalt-fibers-alternative-to-glass> (accessed June
2 16, 2020).
- 3 [10] Mason K. The still-promised potential of basalt fiber composites. *Compos World* 2020.
4 [https://www.compositesworld.com/articles/the-still-promised-potential-of-basalt-fiber-](https://www.compositesworld.com/articles/the-still-promised-potential-of-basalt-fiber-composites)
5 [composites](https://www.compositesworld.com/articles/the-still-promised-potential-of-basalt-fiber-composites) (accessed June 16, 2020).
- 6 [11] Fiore V, Scalici T, Di Bella G, Valenza A. A review on basalt fibre and its composites. *Compos*
7 *Part B Eng* 2015;74:74–94. <https://doi.org/10.1016/j.compositesb.2014.12.034>.
- 8 [12] Dhand V, Mittal G, Rhee KY, Park SJ, Hui D. A short review on basalt fiber reinforced polymer
9 composites. *Compos Part B Eng* 2015;73:166–80.
10 <https://doi.org/10.1016/j.compositesb.2014.12.011>.
- 11 [13] Wei B, Cao H, Song S. Degradation of basalt fibre and glass fibre/epoxy resin composites in
12 seawater. *Corros Sci* 2011;53:426–31. <https://doi.org/10.1016/j.corsci.2010.09.053>.
- 13 [14] Fiore V, Di Bella G, Valenza a. Glass–basalt/epoxy hybrid composites for marine applications.
14 *Mater Des* 2011;32:2091–9. <https://doi.org/10.1016/j.matdes.2010.11.043>.
- 15 [15] Davies P, Verbouwe W. Evaluation of Basalt Fibre Composites for Marine Applications. *Appl*
16 *Compos Mater* 2018;25:299–308. <https://doi.org/10.1007/s10443-017-9619-3>.
- 17 [16] Jaksic V, Wallace F, Ó Brádaigh CM. Upscaling of Tidal Turbine Blades: Glass or Carbon Fibre
18 Reinforced Polymers? *Proc. Twelfth Eur. Wave Tidal Energy Conf.*, 2017.
- 19 [17] Pappa EJ, Murray JJ, Walls M, Alam P, Flanagan T, Doyle A, et al. Fatigue life analysis of hybrid
20 E-glass/carbon fibre powder epoxy materials for wind turbine blades. *ECCM 2018 - 18th Eur.*
21 *Conf. Compos. Mater.*, 2018, p. 24–8.
- 22 [18] Murray RE, Swan D, Snowberg D, Berry D, Beach R, Rooney S. Manufacturing a 9-meter
23 thermoplastic composite wind turbine blade. *32nd Tech. Conf. Am. Soc. Compos.* 2017, vol. 1,
24 2017, p. 29–43. <https://doi.org/10.12783/asc2017/15166>.
- 25 [19] Bortolotti P. Carbon glass hybrid materials for wind turbine rotor blades. TU Delft, 2012.
- 26 [20] Ennis B, Kelley C, Naughton B, Norris R, Das S, Lee D, et al. Optimized Carbon Fiber
27 Composites in Wind Turbine Blade Design. 2019.
- 28 [21] Swolfs Y. Perspective for fibre-hybrid composites in wind energy applications. *Materials*
29 (Basel) 2017;10. <https://doi.org/10.3390/ma10111281>.
- 30 [22] Nijssen RPL, Brøndsted P. Fatigue as a design driver for composite wind turbine blades. 2013.
31 <https://doi.org/10.1533/9780857097286.2.175>.
- 32 [23] Fagan EM, Wallace F, Jiang Y, Kazemi A, Goggins J. Design and testing of a full-scale 2 MW
33 tidal turbine blade. *Proc. 13th Eur. Wave Tidal Energy Conf.*, vol. 33, Naples: 2019.
- 34 [24] Sutcliffe MPF, Lemanski SL, Scott AE. Measurement of fibre waviness in industrial composite
35 components. *Compos Sci Technol* 2012;72:2016–23.
36 <https://doi.org/10.1016/j.compscitech.2012.09.001>.
- 37 [25] Wieland B, Ropte S. Process Modeling of Composite Materials for Wind-Turbine Rotor Blades:
38 Experiments and Numerical Modeling. *Materials (Basel)* 2017;10:1157–69.
39 [https://doi.org/https://doi.org/10.3390/ma10101157](https://doi.org/10.3390/ma10101157).
- 40 [26] Kim D, Centea T, Nutt SR. Modelling and monitoring of out-time and moisture absorption
41 effects on cure kinetics and viscosity for an out-of-autoclave (OoA) prepreg. *Compos Sci*

- 1 Technol 2017;138:201–8.
2 <https://doi.org/https://doi.org/10.1016/J.COMPSCITECH.2016.11.023>.
- 3 [27] Radanitsch J. Multi-layered Carbon Stacks for Large Wind Turbine Blades. Proc. CAMX 2014,
4 Orlando, FL, USA: 2014.
- 5 [28] Cheney M. C., Migliore P. G. Feasibility Study of Pultruded Blades for Wind Turbine Rotors.
6 Wind Eng 1999;23:145–58.
- 7 [29] O’Leary K, Pakrashi V, Kelliher D. Optimization of composite material tower for offshore wind
8 turbine structures. Renew Energy 2019;140:928–42.
9 <https://doi.org/10.1016/j.renene.2019.03.101>.
- 10 [30] Maguire JM, Nayak K, Ó Brádaigh CM. Characterisation of epoxy powders for processing
11 thick-section composite structures. Mater Des 2018;139:112–21.
12 <https://doi.org/10.1016/J.MATDES.2017.10.068>.
- 13 [31] Maguire JM, Simacek P, Advani SG, Ó Brádaigh CM. Novel epoxy powder for manufacturing
14 thick-section composite parts under vacuum-bag-only conditions. Part I: Through-thickness
15 process modelling. Compos Part A Appl Sci Manuf 2020;136.
16 <https://doi.org/https://doi.org/10.1016/j.compositesa.2020.105969>.
- 17 [32] Maguire JM, Nayak K, Ó Brádaigh CM. Novel epoxy powder for manufacturing thick-section
18 composite parts under vacuum-bag-only conditions. Part II: Experimental validation and
19 process investigations. Compos Part A Appl Sci Manuf 2020;136.
20 <https://doi.org/https://doi.org/10.1016/j.compositesa.2020.105970>.
- 21 [33] Mamalis D, Flanagan T, Ó Brádaigh CM. Effect of fibre straightness and sizing in carbon fibre
22 reinforced powder epoxy composites. Compos Part A Appl Sci Manuf 2018;110:93–105.
23 <https://doi.org/https://doi.org/10.1016/j.compositesa.2018.04.013>.
- 24 [34] Murray JJ, Pappa EJ, Mamalis D, Breathnach G, Doyle A, Flanagan T, et al. Characterisation of
25 carbon fibre reinforced powder epoxy composites for wind energy blades. Proc. 18th Eur.
26 Conf. Compos. Mater., Athens, Greece: 2018.
- 27 [35] Mamalis D, Murray JJ, McClements J, Tsikritsis D, Koutsos V, McCarthy ED, et al. Novel
28 carbon-fibre powder-epoxy composites: Interface phenomena and interlaminar fracture
29 behaviour. Compos Part B Eng 2019;107012.
30 <https://doi.org/10.1016/J.COMPOSITESB.2019.107012>.
- 31 [36] Grogan D, Flanagan M, Walls M, Leen S, Doyle A, Harrison N, et al. Influence of
32 microstructural defects and hydrostatic pressure on water absorption in composite materials
33 for tidal energy. J Compos Mater 2018;52:2899–917.
34 <https://doi.org/https://doi.org/10.1177/0021998318755428>.
- 35 [37] Finnegan W, Glennon C, Kelly G, Maguire J, Flanagan M. Manufacture of High Performance
36 Tidal Turbine Blades using Composite Materials. 13th Eur. Wave Tidal Energy Conf., Naples:
37 2019.
- 38 [38] Gherlone L, Rossini T, Stula V. Powder coatings and differential scanning calorimetry: the
39 perfect fit. Prog Org Coatings 1998;34:57–63. [https://doi.org/https://doi.org/10.1016/S0300-9440\(98\)00039-3](https://doi.org/https://doi.org/10.1016/S0300-9440(98)00039-3).
- 40
- 41 [39] Sharma S, Luzinov I. Ultrasonic curing of one-part epoxy system. J Compos Mater
42 2011;45:2217–24. <https://doi.org/https://doi.org/10.1177/0021998311401075>.
- 43 [40] Ó Brádaigh CM, Doyle A, Doyle D, Feerick PJ. Electrically-Heated Ceramic Composite Tooling

- 1 for Out-of-Autoclave Manufacturing of Large Composite Structures. SAMPE J 2011;47.
- 2 [41] Edie D., Lickfield GC, Allen LE, McCollum JR. Thermoplastic Coating of Carbon Fibres.
3 Hampton, VA, USA: 1989.
- 4 [42] Bayha TD, Osborne PP, Thrasher TP, Hartness JT, Johnston NJ, Marchello JM, et al. Processing,
5 Properties and Applications of Composites Using Powder-Coated Epoxy Towpreg Technology.
6 Proc. NASA's 4th Adv. Compos. Technol. Conf., Salt Lake City, Utah: 1993.
- 7 [43] Ramasamy A, Wang Y, Muzzy J. Braided thermoplastic composites from powder-coated
8 towpregs. Part I: Towpreg characterization. Polym Compos 1996;17:497–504.
9 <https://doi.org/https://doi.org/10.1002/pc.10639>.
- 10 [44] Allred RE, Wesson SP, Babow DA. Powder Impregnation Studies for High Temperature
11 Towpregs. SAMPE J 2004;40:40–8.
- 12 [45] Nunes JP, van Hattum FWJ, Bernardo CA, Brito AM, Pouzada AS, Silva JF, et al. Chapter 11
13 Production of Thermoplastic Towpregs and Towpreg- Based Composites. Polym. Compos.
14 from Nano- to Macroscale, 2005, p. 189–213.
- 15 [46] Stone KR, Springer JJ. Advanced Composites Technology Case Study at NASA Langley
16 Research Center. 1995.
- 17 [47] Padaki S, Drzal LT. A Consolidation Model for Polymer Powder Impregnated Tapes. J Compos
18 Mater 1997;31:2202-2227[1] S. Padaki, L.T. Drzal, A Consolidatio.
19 <https://doi.org/10.1177/002199839703102105>.
- 20 [48] Nunes JP, Silva JF, Novo PJ. Processing Thermoplastic Matrix Towpregs by Pultrusion. Adv
21 Polym Technol 2013;32:E306–12. <https://doi.org/10.1002/adv.21279>.
- 22 [49] Robert C, Mamalis D, Alam P, Lafferty AD, Ó Cadhain C, Breathnach G, et al. Powder Epoxy
23 Based UD-CFRP Manufacturing Routes For Turbine Blade Application. Proc. SAMPE Eur. Conf.
24 '18, Southampton, UK: 2018.
- 25 [50] Robert C, Pecur T, McCarthy ED, Ó Brádaigh CM. Tidal turbine blade composites using basalt
26 fibre. 22nd Int. Conf. Compos. Mater., Melbourne: 2019.
- 27 [51] Yang P, Varughese B, Muzzy JD. Flexible thermoset towpregs by electrostatic powder fusion
28 coating. Proc. 36th Int. SAMPE Symp. Exhib., San Diego, USA: 1991.
- 29 [52] Nunes JP, Bernardo CA, Pouzada AS, Edie DD. Modeling of the consolidation of
30 polycarbonate/carbon fiber towpregs. Polym Compos 1999;20:260–8.
31 <https://doi.org/10.1002/pc.10353>.
- 32 [53] Flanagan MH, Doyle F, Fagan E, Goggins J, Leen SB, Doyle A, et al. Large Scale Structural
33 Testing of Wind Turbine Blades Manufactured Using a One- Shot Out-Of-Autoclave Process.
34 Proc Civ Eng Res Irel Conf 2016.
- 35 [54] Fagan EM, Flanagan M, Leen SB, Flanagan T, Doyle A, Goggins J. Physical experimental static
36 testing and structural design optimisation for a composite wind turbine blade. Compos Struct
37 2017;164:90–103. <https://doi.org/10.1016/J.COMPSTRUCT.2016.12.037>.
- 38 [55] Damiano M, D'Ettore A. Structural design of a multi-megawatt wind turbine blade with ONE
39 SHOT BLADE® Technology. J. Phys. Conf. Ser., vol. 1037, 2018. <https://doi.org/10.1088/1742-6596/1037/4/042002>.
- 40
- 41 [56] Toray Carbon Fibers America. T700S Data Sheet. 2019.

- 1 [57] Basaltex. Standard Portfolio - Rovings, Twisted Yarns & Chopped Fibers. 2000.
- 2 [58] Basaltex. Basaltex Basic Fibre Properties TDS. 2018.
- 3 [59] Mafic. Assembled Roving TDS. 2018.
- 4 [60] Padaki S, Drzal LT. A simulation study on the effects of particle size on the consolidation of
5 polymer powder impregnated tapes. *Compos Part A Appl Sci Manuf* 1999;30:325–37.
6 [https://doi.org/https://doi.org/10.1016/S1359-835X\(98\)00115-8](https://doi.org/https://doi.org/10.1016/S1359-835X(98)00115-8).
- 7 [61] Allred RE, Wesson SP, Gordon B. Real Time Process Control of Polymer Loading on Powder
8 Towpreg. SAMPE Conf., Baltimore, USA: 2009.
- 9 [62] Garcia Nava R. Pilot Powder Impregnation Line for Carbon-Fibre Unidirectional Tape. The
10 University of Edinburgh, 2016.
- 11 [63] Woolard DE, Ramani K. Electric field modeling for electrostatic powder coating of a
12 continuous fiber bundle. *J Electrostat* 1995;35:373–87.
13 [https://doi.org/https://doi.org/10.1016/0304-3886\(95\)00029-A](https://doi.org/https://doi.org/10.1016/0304-3886(95)00029-A).
- 14 [64] Naskar AK, Edie DD. Consolidation of Reactive Ultem® Powder-coated Carbon Fiber Tow for
15 Space Structure Composites by Resistive Heating. *J Compos Mater* 2006;40:1871–83.
16 <https://doi.org/10.1177/0021998306061300>.
- 17 [65] Hayes SA, Lafferty AD, Altinkurt G, Wilson PR, Collinson M, Duchene P. Direct electrical cure
18 of carbon fiber composites. *Adv Manuf Polym Compos Sci* 2015;1:112–9.
19 <https://doi.org/10.1179/2055035915Y.0000000001>.
- 20 [66] Dugger JA, Hirt DE. PMR-15/carbon fiber composites produced from powder-coated towpreg.
21 *Polym Compos* 1996;17:492–6. <https://doi.org/10.1002/pc.10638>.
- 22 [67] Parasnis NC, Ramani K, Borgaonkar HM. Ribbonizing of electrostatic powder spray
23 impregnated thermoplastic tows by pultrusion. *Compos Part A Appl Sci Manuf* 1996;27:567–
24 74. [https://doi.org/10.1016/1359-835X\(96\)00017-6](https://doi.org/10.1016/1359-835X(96)00017-6).
- 25 [68] Brown JH, Colton JS. A machine system for the rapid production of composite structures.
26 *Polym Compos* 2000;21:124–33. <https://doi.org/10.1002/pc.10171>.
- 27 [69] Novo PJ, Silva JF, Nunes JP, Marques AT. Pultrusion of fibre reinforced thermoplastic pre-
28 impregnated materials. *Compos Part B Eng* 2016;89:328–39.
29 <https://doi.org/https://doi.org/10.1016/j.compositesb.2015.12.026>.
- 30 [70] Miller A, Wei C, Gibson AG. Manufacture of polyphenylene sulfide (PPS) matrix composites
31 via the powder impregnation route. *Compos Part A Appl Sci Manuf* 1996;27:49–56.
32 [https://doi.org/https://doi.org/10.1016/1359-835X\(95\)00010-Y](https://doi.org/https://doi.org/10.1016/1359-835X(95)00010-Y).
- 33 [71] Kratmann K, Sutcliffe M, Lilleheden L, Pyrz R, Thomsen O. A novel image analysis procedure
34 for measuring fibre misalignment in unidirectional fibre composites. *Compos Sci Technol*
35 2009;69:228–38. <https://doi.org/10.1016/j.compscitech.2008.10.020>.
- 36 [72] Wang J, Potter KD, Etches J. Experimental investigation and characterisation techniques of
37 compressive fatigue failure of composites with fibre waviness at ply drops. *Compos Struct*
38 2013;100:398–403. <https://doi.org/10.1016/j.compstruct.2013.01.010>.
- 39 [73] Mehdikhani M, Gorbatikh L, Verpoest I, Lomov S V. Voids in fiber-reinforced polymer
40 composites: A review on their formation, characteristics, and effects on mechanical
41 performance. *J Compos Mater* 2019;53:1579–669.
42 <https://doi.org/10.1177/0021998318772152>.

- 1 [74] BS EN ISO 527-5. Plastics — Determination of tensile properties - Part 5: Test conditions for
2 unidirectional fibre-reinforced plastic composites. 2009.
3 <https://doi.org/10.1016/j.fertnstert.2015.12.022>.
- 4 [75] BS EN ISO 14125. Fibre-reinforced plastic composites — Determination of flexural properties.
5 1998.
- 6 [76] ASTM D6641/D6641M - 16E1. Standard Test Method for Compressive Properties of Polymer
7 Matrix Composite Materials Using a Combined Loading Compression (CLC) Test Fixture. 2016.
- 8 [77] Centea T, Grunenfelder LK, Nutt SR. A review of out-of-autoclave prepregs – Material
9 properties, process phenomena, and manufacturing considerations. *Compos Part A Appl Sci*
10 *Manuf* 2015;70:132–54. <https://doi.org/10.1016/j.compositesa.2014.09.029>.
- 11 [78] Gutowski TG, Cai Z, Bauer S, Boucher D, Kingery J, Wineman S. Consolidation Experiments for
12 Laminate Composites. *J Compos Mater* 1987;21:650–69.
13 <https://doi.org/10.1177/002199838702100705>.
- 14 [79] Röchling. Pultruded profiles for spar caps 2020. [https://www.roechling-](https://www.roechling-industrial.com/uk/industries/renewable-energies/plastics-for-wind-energy/materials-for-wind-turbine-blades/spar-caps-for-wind-turbines)
15 [industrial.com/uk/industries/renewable-energies/plastics-for-wind-energy/materials-for-](https://www.roechling-industrial.com/uk/industries/renewable-energies/plastics-for-wind-energy/materials-for-wind-turbine-blades/spar-caps-for-wind-turbines)
16 [wind-turbine-blades/spar-caps-for-wind-turbines](https://www.roechling-industrial.com/uk/industries/renewable-energies/plastics-for-wind-energy/materials-for-wind-turbine-blades/spar-caps-for-wind-turbines) (accessed June 1, 2020).
- 17 [80] Legault M. Wind blade spar caps: Pultruded to perfection? *Compos World* 2018.
- 18 [81] ZOLTEK. Technical Datasheet PX35 Continuous Tow. 2020.
- 19 [82] Gurit. Carbon & Glass SparPreg™ Full General Datasheet. 2016.
- 20 [83] ZOLTEK. Technical Datasheet PX35 Pultruded Profiles. 2020.
- 21 [84] Wang M, Zhang Z, Li Y, Li M, Sun Z. Chemical durability and mechanical properties of alkali-
22 proof basalt fiber and its reinforced epoxy composites. *J Reinf Plast Compos* 2008;27:393–
23 407. <https://doi.org/10.1177/0731684407084119>.
- 24 [85] Potter K, Khan B, Wisnom M, Bell T, Stevens J. Variability, fibre waviness and misalignment in
25 the determination of the properties of composite materials and structures. *Compos Part A*
26 *Appl Sci Manuf* 2008;39:1343–54. <https://doi.org/10.1016/j.compositesa.2008.04.016>.
- 27 [86] Solvay. Cycom® 5276-1 Technical Data Sheet. 2019.
- 28 [87] Hexcel. HexPly® 8552 Product Data Sheet. 2020.
- 29 [88] Floreani C, Robert C, Alam P, Davies P, Ó Brádaigh CM. Characterization of mode I
30 interlaminar properties of novel composites for tidal turbine blades. 13th Eur. Wave Tidal
31 Energy Conf., Naples: 2019.

32